© 2023. Published by The Company of Biologists Ltd | Journal of Experimental Biology (2023) 226, jeb245383. doi:10.1242/jeb.245383

RESEARCH ARTICLE

Impacts of ocean acidification and warming on post-larval growth and metabolism in two populations of the great scallop (*Pecten maximus*)

Ewan Harney[1,2,*,‡], Samuel P. S. Rastrick[3], Sebastien Artigaud[1], Julia Pisapia[2], Benoit Bernay[4], Philippe Miner[2], Vianney Pichereau[1], Øivind Strand[3], Pierre Boudry[5] and Gregory Charrier[1]

ABSTRACT

Ocean acidification and warming are key stressors for many marine organisms. Some organisms display physiological acclimatization or plasticity, but this may vary across species ranges, especially if populations are adapted to local climatic conditions. Understanding how acclimatization potential varies among populations is therefore important in predicting species responses to climate change. We carried out a common garden experiment to investigate how different populations of the economically important great scallop (*Pecten maximus*) from France and Norway responded to variation in temperature and P_{CO_2} concentration. After acclimation, post-larval scallops (spat) were reared for 31 days at one of two temperatures (13°C or 19°C) under either ambient or elevated P_{CO_2} (pH 8.0 and pH 7.7). We combined measures of proteomic, metabolic and phenotypic traits to produce an integrative picture of how physiological plasticity varies between the populations. The proteome of French spat showed significant sensitivity to environmental variation, with 12 metabolic, structural and stress-response proteins responding to temperature and/or P_{CO_2}. Principal component analysis revealed seven energy metabolism proteins in French spat that were consistent with countering ROS stress under elevated temperature. Oxygen uptake in French spat did not change under elevated temperature but increased under elevated P_{CO_2}. In contrast, Norwegian spat reduced oxygen uptake under both elevated temperature and P_{CO_2}. Metabolic plasticity allows French scallops to maintain greater energy availability for growth compared with Norwegian spat. However, increased physiological plasticity and growth in French spat may come at a cost, as they showed reduced survival compared with Norwegian scallops under elevated temperature.

KEY WORDS: Bivalve, Proteomics, Trade-offs, Calcification, Climate change, Physiological plasticity

[1]Univ Brest, CNRS, IRD, Ifremer, UMR 6539, LEMAR, IUEM-UBO, 29280 Plouzané, France. [2]Ifremer Centre Bretagne, LEMAR UMR 6539, 29280 Plouzané, France. [3]Institute of Marine Research (IMR), Nordnes, 5817 Bergen, Norway. [4]Platform Proteogen, SF ICORE 4206, Caen-Normandy University, 14032 Caen, France. [5]Département Ressources Biologiques et Environnement, Ifremer Centre Bretagne, 29280 Plouzané, France.
*Present address: Institute of Evolutionary Biology (CSIC-UPF), Passeig Marítim de la Barceloneta, 08003 Barcelona, Spain.

‡Author for correspondence (ewan.harney@gmail.com)

E.H., 0000-0003-0680-3253; B.B., 0000-0002-3624-1514; V.P., 0000-0003-1078-9407; ØS., 0000-0001-9594-5928; P.B., 0000-0002-5150-2276; G.C., 0000-0002-8730-9267

Received 7 December 2022; Accepted 2 May 2023

INTRODUCTION

Elevated atmospheric CO_2 is a major driver of global climate change (Crowley and Berner, 2001), causing surface temperatures to rise both on land and in the ocean (Hansen et al., 2006). Oceans act as a sink for more than a third of all anthropogenic carbon emissions (Sabine et al., 2004), leading to changes in marine carbonate chemistry and acidification of marine environments (Caldeira and Wickett, 2003; Doney et al., 2009). Changes in temperature and P_{CO_2} exert strong impacts on populations of ectothermic marine organisms (Pörtner, 2002; Brierley and Kingsford, 2009), especially those organisms that construct their shells from calcium carbonate (Ries et al., 2009). Furthermore, when experienced simultaneously, ocean acidification and warming (OAW) can result in synergistic or unforeseen effects (Pörtner and Farrell, 2008; Todgham and Stillman, 2013; Davis et al., 2013).

Phenotypic responses to OAW depend on the integration of various molecular changes into physiological responses and physical traits (Pörtner, 2012). Changes at the molecular, physiological and physical trait level vary greatly amongst species (Kroeker et al., 2013; Okazaki et al., 2017) and even within species (Morley et al., 2009; Pespeni et al., 2013a; Dam, 2013; Calosi et al., 2017; Vargas et al., 2017). This variation may contribute towards phenotypic evolution, assuming that it has a heritable basis (Pespeni et al., 2013b; Dam et al., 2021). One of the key selective factors that could drive local adaptation is temperature variation along latitudinal gradients (Pereira et al., 2017). For example, towards lower latitude (warmer) range edges, populations may live close to their thermal limits (Pereira et al., 2017), and increases in temperature may induce poleward range shifts (Hale et al., 2017). Ectotherms from more thermally variable (temperate and boreal) latitudes may have greater thermal tolerance and ability to acclimatize than those from thermally stable (polar and equatorial) latitudes (Sunday et al., 2011). Furthermore, populations from higher latitude (colder) range edges may be less able to adjust their metabolism under elevated P_{CO_2} (Calosi et al., 2017) and suffer reduced metabolism under combined stresses (Di Santo, 2016). Yet, because metabolic rates increase exponentially with temperature, a given range of metabolic rates occupies a narrower range of temperatures in warmer climes (Payne and Smith, 2017), which could allow for greater acclimatization potential in cooler parts of the range. The fact that congeneric species can differ in how they adjust metabolism along their latitudinal distributions (Whiteley et al., 2011; Rastrick and Whiteley, 2013) reinforces the importance of studying evolved differences in response to environmental variation.

Metabolism is therefore a key determinant of response potential to environmental variation among marine ectotherms. The ability to maintain oxygen supply is crucial for physiological performance

(Byrne, 2011; Pörtner, 2012) and determining allocation of resources to competing energetic demands (Sokolova et al., 2012), with consequences for life history traits such as growth and fecundity. Chronic temperature stress frequently leads to elevated metabolic rates (Lefevre, 2016) but can also result in acclimatization and maintenance of 'normal' metabolic rates (Seebacher et al., 2010) or reduced metabolism (Anestis et al., 2008; Clark et al., 2013). Effects of increased P_{CO_2} on metabolism also appear variable (Lefevre, 2016) and may differ across life stages (Pörtner et al., 2010). In the long-term, calcifying organisms generally increase their metabolic rate in acidified conditions (Rastrick et al., 2018) or when warming and acidification are experienced simultaneously (e.g. Matoo et al., 2013) but the physiological response may be dependent on the mechanisms and costs of maintaining acid–base status (Small et al., 2015).

Changes in both temperature and P_{CO_2} are perceived and interpreted via a wide range of cellular signalling and metabolic pathways, which then facilitate acclimatization via physiological plasticity (Seebacher et al., 2010; Pörtner, 2012; Hurd et al., 2020). This acclimatization is likely to play a key role in shaping tolerance to environmental stress (Seebacher et al., 2015), although it may also limit local adaptation (Sanford and Kelly, 2011). Our understanding of the molecular mechanisms underlying acclimatization has been aided by the development of high-throughput 'omics technologies (Mykles et al., 2010), including environmental proteomics (Tomanek, 2011), which can reveal multifaceted responses to variation in the environment and climate stress. Relating proteomic responses to energetic trade-offs and, in turn, to complex phenotypes (such as rates of growth, development and survival), can provide clues about potential links between molecular responses and their fitness consequences (Artigaud et al., 2015; Harney et al., 2016; Timmins-Schiffman et al., 2020). Meanwhile, comparisons of congeners or different populations can reveal functionally adaptive patterns of protein abundance (Fields et al., 2012; Tomanek, 2014). Integration of responses across molecular (e.g. proteomic), physiological, phenotypic and population scales is necessary to best predict how species will respond to global climate change (Pörtner et al., 2006; Pörtner, 2012).

It is generally accepted that molluscs are particularly at risk from ocean acidification and warming (Harvey et al., 2013; Kroeker et al., 2013), even though molluscan taxa differ in their susceptibility. Among bivalves, scallops may be more tolerant to acidification than oysters and mussels (Scanes et al., 2014) and appear to adjust their metabolism under combined stresses (Götze et al., 2020). Populations of great (or king) scallop *Pecten maximus* from temperate waters appear better able to maintain acid–base homeostasis compared with those from boreal waters (Schalkhausser et al., 2013, 2014), yet the molecular mechanisms that confer this tolerance and the phenotypic consequences of chronic exposure to elevated temperature and P_{CO_2} remain poorly understood. Globally, scallop fisheries represent important economic resources, and successfully managing this resource requires a better understanding of how OAW will impact scallops at the population level (Rheuban et al., 2018). In the north-eastern Atlantic, *P. maximus* is an economically important species that is exploited along its native range, from Norway to Spain (Duncan et al., 2016). Interestingly, *P. maximus* from Norway appear to be genetically distinct from other European populations (Morvezen et al., 2016; Vendrami et al., 2019), and adults from the Bay of Brest in France and the North Sea near the western fjords of Norway display differences in growth phenotypes (Chauvaud et al., 2012) and proteomic profile (Artigaud et al., 2014b).

Such differences may reflect environmental variation between the sites where these individuals were sampled. Mean sea surface temperature (SST) is higher in the Bay of Brest (BoB: 13.2°C) than it is in the North Sea near the western fjords (NS: 10.3°C), although the August maximum is comparable and the annual range is larger in NS (4.2–16.9°C) than BoB (9.5–16.9°C) [Coriolis Cotier (https://data.coriolis-cotier.org/platform/6200450); Institute for Marine Research (http://www.imr.no/forskning/forskningsdata/stasjoner/view/initdownload)]. Furthermore, mean surface P_{CO_2} values are higher in BoB (421 µatm) than NS (337 µatm) and show a greater annual range in BoB (BoB: 334-495 µatm, NS: 296-371 µatm) (Coriolis Cotier; Omar et al., 2019; Abdirahman Omar, NORCE Norwegian Research Centre pers. comm.). Other environmental factors such as salinity are also known to differ between the sites, which is on average higher in BoB (BoB: 34.4 ppt; NS: 31.2 ppt) but more variable annually in NS (BoB: 33.2–35.1 ppt; NS: 29.2–32.5 ppt) (Coriolis Cotier; Institute for Marine Research); annual variation in conditions is shown in data available on figshare (doi:10.6084/m9.figshare.22226239.v3). Thus, it is not clear how much the observed phenotypic (Chauvaud et al., 2012) and proteomic (Artigaud et al., 2014b) differences between the two populations are due to environmental variation between the sites or genetic divergence. Determining whether phenotypic and proteomic differences between these two populations are genetically fixed or arise from plastic responses to environmental variation is therefore an important step in determining whether these traits are heritable and could have an adaptive basis. To improve our understanding of how *P. maximus* populations might respond to future climate change, we carried out common garden experiments in the lab using juvenile *P. maximus* (known as spat) from French and Norwegian populations. Understanding how changing environmental conditions affect sensitive early life stages is of particular importance, because these represent a bottleneck for population persistence (Byrne, 2012). Spat were reared at three temperatures and two P_{CO_2} concentrations (6 treatments) over a 5 week period and phenotypic responses were measured at multiple levels of biological organization, including protein abundance, oxygen consumption and growth in soft tissue and calcified structures.

MATERIALS AND METHODS

Production of *Pecten maximus* spat

For the first few months after metamorphosis, post-larval *Pecten maximus* (Linnaeus 1758) are commonly known as spat (although there is no further developmental transition before maturation, they are only referred to as juveniles after the first year; Christophersen et al., 2008). To test how spat respond to increased temperatures and P_{CO_2}, we carried out a common garden experiment at the experimental facilities of Ifremer Centre Bretagne (Plouzané, France). Both Norwegian and French spat were obtained from commercial scallop hatcheries (Scalpro AS, 5337, Rong, Vestland, Norway and Écloserie du Tinduff, Port du Tinduff 29470, Plougastel Daoulas, Brittany, France). At these hatcheries, adults collected in the wild are induced to spawn and offspring are reared from fertilized eggs through to early spat, before being transferred to sea cages to complete this phase of growth. Because of limitations on the availability of spat and differences in hatchery practices, Norwegian and French spat varied in their developmental history at the start of the experiment. Norwegian spat (offspring of approximately 60 adults sampled near Bergen, Norway) were approximately 7 months old and had yet to be placed in sea cages, while French Spat (offspring of approximately 30 adults sampled in the Rade de Brest, France) were 3 months old and had spent 2 weeks

in sea cages. Spat were obtained in June and the experiment ran until the end of July. In June SST conditions are colder in the North Sea (12.2°C) than in the Bay of Brest (15.1°C), although by August, SST is similar in the two locations (16.9°C).

Transport of approximately 3000 Norwegian spat from the hatchery in Rong, Norway to the experimental facility at Ifemer, Centre de Bretagne, France, followed the recommendations of Christophersen et al. (2008) and took approximately 12 h. Transport was carried out following submission and approval of an EU intra-trade certificate submitted via the TRACES platform. Spat were removed from their tanks and transferred to a cooled container (11°C) containing seawater-soaked absorbent paper for road transport to Bergen airport and air transport to Paris. On arrival in Paris, spat were transferred to a large (1000 liter) tank containing seawater (maintained at 13°C in a refrigerated van). From here, they were transported to the experimental facility and transferred to tanks maintained at 13°C.

Approximately 9000 French spat were collected from sea cages near Sainte-Anne du Portzic, in the Bay of Brest, 6 days after the transport of Norwegian spat. We replicated the most stressful part of the transportation of Norwegian spat (emersion for approximately 6 h) for French spat before introducing them to tanks.

Characterization of experimental system and animal maintenance

Following transport or simulated transport, spat were transferred to six 'raceway' flow through tanks (100 liters). For each population, spat were split among 18 mesh-bottomed trays (mesh 500 µm), held approximately 2.5 cm from the tank bottom by PVC supports, with populations kept separate initially (6 trays per raceway, 36 total trays). Each raceway drained into an independent header tank (30 liters) containing an overflow. The rate of water renewal was regulated by gravity pressure between the input and overflow: filtered UV-sterilized sea water was supplied at a flow of approximately 90 ml min^{-1}, leading to approximately one renewal per day. Header tanks also received a constant flow of microalgae (equal concentrations of *Tisochrysis lutea* and *Chaetoceros gracilis* at a final concentration of approximately 80,000 cells ml^{-1} in experimental tanks), which was supplied to two different header tanks from 10 liter bottles via peristaltic pumps (two delivery tubes per pump, one for each header tank). Bottles of algae were replenished every 2 days.

From each header tank, a submerged pump supplied algae-enriched seawater to a network of PVC pipes (with small holes drilled in them) overhanging each mesh-bottomed tray in the raceway at a rate of about 400 l h^{-1}or approximately 66 l h^{-1} per tray. Hereafter we refer to each interconnected header tank and raceway as an experimental system, or system for short. The six systems were disinfected and rinsed on a weekly basis, with spat trays transferred to small tanks during cleaning (<30 min per system). During cleaning, dead individuals (those with their valves clearly open and unresponsive to tactile and visual stimuli) and empty shells were removed from trays. We also removed individuals that were clearly dead during frequent inspections of the trays (5 days a week) (see fig. A2 in figshare: doi:10.6084/m9.figshare.22226239.v3).

Spat were acclimated for 10 days (Norwegian spat) or 6 days (French spat) at 14.2±0.5°C (ambient P_{CO_2}). Then, during an adjustment period of 6 days, temperatures were slowly changed in all six systems to reach treatment conditions (Fig. S1A), nominally 13, 16 and 19°C (two systems at each temperature). Temperatures in the 16 and 19°C systems were increased using resistance heaters placed in header tanks, temperatures in the 13°C systems were reduced by decreasing the temperature of in-flowing water. During acclimation and the initial part of the adjustment period, each raceway housed trays of a single population. On the penultimate day of the adjustment period, raceways were rearranged such that each contained an alternating sequence of Norwegian and French spat (three trays of each). The concentration of P_{CO_2} was then elevated for one system at each temperature by bubbling CO_2 through a CO_2 reactor (JBL GmbH & Co. KG, Neuhofen, Germany) in the header tank. Elevated P_{CO_2} was maintained by negative feedback based on a target pH of 7.7 (compared with 8.0 in untreated tanks), in line with end-of-the century predictions under representative concentration pathway (RCP) 8.5 (IPCC, 2022). Experimental treatments were maintained for 31 days (hereafter referred to as days 0–31; Fig. S1A,B). We hereafter use the nominal target temperatures and the abbreviations normCO$_2$ (normal P_{CO_2}, pH 8.0) and highCO$_2$ (high P_{CO_2}, pH 7.7) when referring to the different treatments (13-normCO$_2$, 13-highCO$_2$, 16-normCO$_2$, 16-highCO$_2$, 19-normCO$_2$, and 19-highCO$_2$).

Temperature was measured with a digital temperature probe and pH was measured using a WTW pH 340i fitted with a WTW SenTix 41 pH electrode (WTW GmbH, Weilheim, Germany). During acclimation and adjustment, conditions in header tanks were checked daily (excluding weekends), and during the experimental treatment, conditions were monitored twice daily (and once every 2 days during the weekend). Mean temperature and pH values for the six treatments are shown in Table 1 and Fig. S1C,D.

At two points during the experiment (days 23 and 31) duplicated water samples from each experimental system were collected for salinity and alkalinity analyses. Salinity was determined using a refractometer and was found to be 36 PSU in all samples. Alkalinity was determined from bicarbonate ion [HCO_3^-] titration (analyses performed by Labocea laboratories, France). Bicarbonate concentration and pH were used to determine dissolved inorganic carbon (DIC) concentration. DIC, temperature, pH and salinity values were entered into the CO2SYS v.2.1 macro (https://cdiac.ess-dive.lbl.gov/ftp/co2sys/CO2SYS_calc_XLS_v2.1/) to calculate P_{CO_2}, total alkalinity, and saturation states of calcite and aragonite. The calculation was based on constants from Cai and Wang (1998) fitted to the NBS pH scale. Mean (±s.d.) carbonate chemistry conditions are shown in Table 1.

Analysis of survival

Survival of spat in each tray was estimated by counting the number of individuals present in photos taken during the experimental treatment. On days 3, 9, 16, 24 and 31 (approximately once per week) photographs were taken of each of the 36 trays (see fig. A3A in figshare: doi:10.6084/m9.figshare.22226239.v3). To have sufficient image resolution, three photographs were taken of each tray and were stitched together afterwards using GIMP (https://www.gimp.org/). All shells in stitched composites (apart from clearly empty shells) were counted using ImageJ software (https://imagej.nih.gov/). Although these measures may have some limitations (such as the inclusion of recently deceased spat, or undercounts if spat were stacked on top of one another), taking photos reduced the handling time and stress for the spat, allowing for an approximation of live spat with minimal disturbance. Survival analysis was carried out with the *coxme* package (https://cran.r-project.org/package=coxme) in R (https://www.r-project.org/), with Tray as a random factor to account for variation between trays within each experimental system. The significance of population and environmental variable effects on survival were tested with Wald

Journal of Experimental Biology (2023) 226, jeb245383. doi:10.1242/jeb.245383

Table 1. Mean (±s.d.) environmental parameters during experimental treatments (days 0–31)

Nominal treatment		Temperature* (°C)	pH*	$[HCO_3^-]$‡ (µmol kg^{-1})	DIC§ (µmol kg^{-1})	A_T§ (µmol kg^{-1})	P_{CO_2}§ (µatm)	Ω Calcite§	Ω Aragonite§
13°C	pH 8.0 Norm. CO_2	13.37±0.38	7.95±0.06	2184±24	2322±33	2462±53	680±50	2.63±0.29	1.68±0.19
	pH 7.7 High CO_2	13.45±0.37	7.70±0.05	2206±29	2317±31	2356±33	1307±86	1.41±0.11	0.90±0.07
16°C	pH 8.0 Norm. CO_2	16.20±0.60	7.93±0.08	2180±10	2324±3	2473±11	740±56	2.79±0.19	1.80±0.12
	pH 7.7 High CO_2	16.20±0.26	7.68±0.05	2214±16	2328±17	2371±22	1449±61	1.48±0.08	0.96±0.05
19°C	pH 8.0 Norm. CO_2	19.12±0.30	7.93±0.06	2219±23	2374±21	2535±16	808±44	3.03±0.12	1.97±0.08
	pH 7.7 High CO_2	19.20±0.39	7.65±0.04	2241±15	2360±16	2401±17	1660±5	1.51±0.02	0.98±0.01

*Temperature and pH were frequently measured (twice daily during weekdays, once per weekend).
‡Replicated bicarbonate ion ($[HCO_3^-]$) measurements took place at two time points (days 23 and 31).
§DIC, dissolved inorganic carbon; A_T, total alkalinity; P_{CO_2}, partial pressure of CO_2; Ω Calcite and Ω Aragonite, calcite and aragonite saturation states. All values were determined using CO2SYS v.2.1.

chi-square tests using the ANOVA function from the car package (https://cran.r-project.org/package=car; Fox and Weisberg, 2011). Because *coxme* does not allow more than two dependent variables to be tested simultaneously, we first tested for differences between French and Norwegian scallops, before comparing the effects of temperature and P_{CO_2} (plus their interaction) on survival for each population separately. Contrasts between groups were evaluated with pairwise *post hoc* tests using the emmeans package (https://cran.r-project.org/package=emmeans). To reduce the effect of sample size differences on statistical power, a random number of French spat, equivalent to the smaller number of Norwegian spat, were included in the survival analysis. Spat (2–6 individuals per tray) were sampled almost daily during the adjustment period and weekly during the experimental treatment for a separate experiment (unpublished data). These individuals were 'left censored' for the purposes of the survival analysis.

Analysis of whole organism phenotypes

At the end of the experiment (day 31), 20–40 individuals were removed from each tray and preserved in 95% ethanol at 4°C. Three primary traits of shell size, shell mass and soft tissue mass were measured for between 8 and 15 individuals from each tray (mean=12). Shell height is one of the most-commonly measured morphological phenotypes in bivalves. Bivalve shells grow by marginal accretion and changes in shell height provide an accurate measure of individual growth. Consistent patterns of accretion in the flat valves of scallops allows the estimation of growth over fine temporal scales (Chauvaud et al., 2012). Soft tissue dry mass (dry body mass) and total shell dry mass (total shell mass) are measures of investment in these two compartments. We also used these measures to estimate the condition index (CI: soft tissue dry mass /shell dry mass ratio), which encapsulates the difference in resource allocation to these compartments (Lucas and Beninger, 1985). Spat were dissected and soft tissue was dried at 75°C for 24 h while both the left valve (flat) and right valve (curved) were air dried for at least 24 h. The dry bodies, flat and curved valves were then weighed to the nearest 0.0001 g using a digital balance (Mettler Toledo).

Multiple high-resolution images of the flat valve at a range of focal depths were obtained using an AxioCam MRC 5 linked to a SteREO Lumar.V12 stereomicroscope (Carl Zeiss) equipped with a motorized stage: the resultant photomosaics were then assembled using AxioVision 4.9.1 software (Carl Zeiss). From these images shell height was measured using ImageJ software (see fig. A3B in figshare: doi:10.6084/m9.figshare.22226239.v3); images were also used to estimate height at the beginning of the experiment (following transport), as growth in the controlled conditions of the experimental facility could be clearly associated with an alteration in the colour of newly calcified shell. Owing to the considerable variation in size among scallops from both populations, initial shell height was included as a covariate in whole organism phenotypic analyses. Although Lucas and Beninger (1985) recommend the use of cubed height as a covariate for mass measures (such that variation scales in the same number of dimensions), we found initial height alone (not raised to a power) better accounted for covariation in the data. Phenotypic measures and ratios were plotted against these initial measures as part of an inspection for outliers. Four out of 431 samples were removed owing to at least one trait showing extreme outlier values. Quantile–quantile plots were assessed to determine probability distributions. Dry body mass and total shell mass were subsequently log transformed to ensure normality. For all analyses, populations were analysed separately because of the strong differences in initial sizes.

The dependency of whole organism phenotypes on temperature, P_{CO_2}, and initial shell dimensions, as well as their 2-way and 3-way interactions, was assessed using linear mixed-effects models in the lme4 package in R (https://cran.r-project.org/package=lme4; Bates et al., 2015); tray was included as a random effect. Backwards stepwise term deletion was used to test the importance of interactions and main effects. Statistics were obtained from minimal models fitted with restricted maximum likelihood and *P*-values were obtained using the lsmeans R package (https://cran.r-project.org/package=lsmeans). When either temperature or the interaction of temperature and P_{CO_2} were significant, contrasts between groups were evaluated with pairwise *post hoc* tests using emmeans. For the interaction between temperature and P_{CO_2}, temperature differences at a given P_{CO_2} and P_{CO_2} differences at a given temperature were considered. Phenotypic responses to temperature and P_{CO_2} were plotted using effect size plots in the jtools package (https://cran.r-project.org/package=jtools) based on fully parameterised linear models (temperature, P_{CO_2}, initial shell dimensions and all interactions). These account for covariate variation (including interactions), include confidence intervals, and can be mean centred. Although they do not account for random

effect variance, these plots provide an intuitive means of visualizing these data when combined with mixed-effects model statistics.

Analysis of metabolic rates

For both populations, the effect of temperature and P_{CO_2} on oxygen consumption ($\dot{M}_{O_2}$), used as a proxy for metabolic rate, was assessed (Rastrick et al., 2018) using randomly selected individuals from highest and lowest temperature treatments (13-normCO_2, 13-highCO_2, 19-normCO_2, 19-highCO_2). On day 27 of the experiment, three spat from each tray (nine per population/treatment combination, n=72) were selected for metabolic analyses.

Spat were placed in individual stop-flow respirometers (volume 100 ml) that were supplied with the same seawater as used for the incubation, oxygenated (above 95% dissolved O_2) and at the same P_{CO_2} and temperature as the animals' respective treatments. Animals were allowed 1 h to recover from handling and regain natural ventilatory behaviour before the flow to each chamber was stopped and the decreases in % oxygen saturation continuously measured using an optical oxygen system (Oxy-10mini, Presence, Labquest 2, Vernier; Rastrick and Whiteley, 2011, Rastrick et al., 2018). Once the chambers were closed, a constant temperature was maintained by use of a water bath. The incubation period was 5 h, during which time, oxygen levels of the seawater did not fall below 70% (% air saturation) to avoid hypoxic conditions. A blank chamber with no animal was used to control for the background respiration in the seawater. The decrease in oxygen (% air saturation) within each chamber was converted to oxygen partial pressure (P_{O_2}) adjusted for atmospheric pressure and vapour pressure adjusted for relative humidity (measured using a multimeter; Labquest 2, Vernier). This decrease in P_{O_2} was converted to concentration by multiplying by the volume of the chamber, minus the animal volume, and the oxygen solubility coefficient adjusted for the effect of temperature and salinity (Benson and Krause, 1984). Values were standardised to individual dry body (tissue) mass and expressed as μmol O_2 h^{-1} mg^{-1}±s.e.m. At the end of these metabolic experiments, the 72 individuals were sacrificed and dissected. Soft tissue was dried and weighed as described for the phenotypic analyses.

$\dot{M}_{O_2}$ values were tested for normality. Although residuals approximated a normal distribution among French spat, they deviated from normality for Norwegian spat. Consequently, the raov function from the package Rfit (https://CRAN.R-project.org/package=Rfit) was used to provide rank-based estimations of linear models. We initially included population, temperature, P_{CO_2} and all possible interactions in this model. However, to facilitate interpretation of the effects of temperature, P_{CO_2} and their interaction, we also fitted models for each population separately. We used Benjamini–Hochberg-adjusted pairwise Wilcoxon tests to identify differences when the interaction was significant.

Analysis of the proteome

Spat for proteomic analyses were collected on day 31 from each tray in the 13-normCO_2, 13-highCO_2, 19-normCO_2 and 19-highCO_2 treatments. For each tray, two samples (each containing a pooled sample of two whole individuals) were flash frozen in liquid nitrogen (48 samples total) and stored at −80°C until analysis. Samples were homogenised by bead beating at 4°C in 500 µl Tris-HCl lysis buffer (100 mmol l^{-1}, pH 6.8) containing 1% Protease Inhibitor Mix (GE Healthcare). We used 2-dimensional gel electrophoresis (2-DE) to analyse protein samples because of its utility in detecting different isoforms of the same protein; isoform differences were previously important in discriminating adult *P. maximus* from these two populations (Artigaud et al., 2014b). A full and detailed description of the protocol for 2-DE and mass-spectrometry of protein samples can be found in Harney et al. (2016), but is described here briefly. Homogenised samples were centrifuged and solubilised proteins from the interphase were quantified using a D_C (detergent compatible) protein assay in a micro-plate reader. Then, 800 µg protein were precipitated and desalted using a 1:1 ratio of sample to TCA/acetone (20% TCA). The supernatant was discarded, and pellets were neutralised by adding Tris-HCl/acetone (80% acetone) containing bromophenol blue as a pH indicator. Pellets were centrifuged once again and air-dried, before being rehydrated in Destreak rehydration solution (GE healthcare) containing 1% IPG (immobilised pH gradient) buffer (pH 4–7). After 1 h, samples were ready for isoelectric focusing (IEF) on the IPGphor3 system (GE healthcare). After IEF, IPG strips were bathed in a rehydration solution (50 mmol l^{-1} Tris–HCl pH 8.8, 6 mol l^{-1} urea, 30% glycerol, 2% SDS and 0.002% Bromophenol Blue) for two 15 min periods, first with 10 mg ml^{-1} dithiothreitol, and then in the same solution containing 48 mg ml^{-1} iodoacetamide. Strips were then deposited on a 15 cm×15 cm lab-cast SDS-PAGE gel containing 12% acrylamide and migrated. Protein spots were stained with Coomassie Blue (PhastGel, GE Healthcare), allowing concentration to be quantified (Noaman and Coorssen, 2018). Gels were bleached with baths of H_2O:methanol:acetic acid (70:30:7) and photographed using G:BOX (SynGene). The 32 clearest gels were taken forward for analysis (4 per population per treatment); detection, background subtraction, normalization and matching of protein spots in the resulting images was carried out using Progenesis SameSpots v.3.3 software (Nonlinear Dynamics, Newcastle upon Tyne, UK) and then manually verified. The effects of population, temperature, and pH were evaluated by running ANOVAs for each spot (combined population analysis). Owing to the large number of tests involved, P-values were adjusted using the false discovery rate (FDR), and fold change values were determined. Proteins which differed significantly in abundance between the populations, or between temperature or P_{CO_2} treatments (FDR≤0.05) were excised from the gels and analysed using mass spectrometry.

Gel pieces were first washed in 50 mmol l^{-1} ammonium bicarbonate (BICAM), and then dehydrated in 100% acetonitrile (ACN). Gel pieces were vacuum-dried, rehydrated with BICAM containing 0.5 µg MS-grade porcine trypsin (Pierce Thermo Scientific), and incubated overnight at 37°C. Peptides were extracted from the gels by alternatively washing with 50 mmol l^{-1} BICAM and ACN, and with 5% formic acid and ACN. Between each washing step, the supernatants from a given gel piece were pooled and finally concentrated by evaporation using a centrifugal evaporator (Concentrator 5301, Eppendorf).

Mass spectrometry (MS) experiments were carried out on an AB Sciex 5800 proteomics analyser equipped with TOF/TOF ion optics and an OptiBeamTM on-axis laser irradiation with 1000 Hz repetition rate. The system was calibrated immediately before analysis with a mixture of Angiotensin I, Angiotensin II, Neurotensin, ACTH clip (1–17) and ACTH clip (18–39), showing that mass precision was above 50 ppm. After tryptic digestion, dry samples were resuspended in 10 µl of 0.1% TFA. A 1 µl volume of this peptide solution was mixed with 10 µl of 5 mg ml^{-1} α-cyano-4-hydroxycinnamic acid matrix prepared in a diluent solution of 50% ACN with 0.1% TFA. The mixture was spotted on a stainless steel Opti-TOF 384 target; the droplet was allowed to evaporate before introducing the target into the mass spectrometer. All acquisitions were taken in automatic mode. A laser intensity of 3400 was

typically employed for ionizing. MS spectra were acquired in the positive reflector mode by summarizing 1000 single spectra (5×200) in the mass range 700–4000 Da. Tandem mass spectrometry (MS/MS) spectra were acquired in the positive MS/MS reflector mode by summarizing a maximum of 2500 single spectra (10×250) with a laser intensity of 4200. For the MS/MS experiments, the acceleration voltage applied was 1 kV and air was used as the collision gas. Gas pressure was set to medium. The fragmentation pattern was used to determine the sequence of the peptide.

Database searching was performed using the MASCOT 2.4.0 program (Matrix Science). A custom database consisting of an EST database from a previous study was used (Artigaud et al., 2014c) and a compilation of the Uniprot database with *P. maximus* as the selected species. The variable modifications allowed were as follows: carbamidomethylation of cystein, K-acetylation, methionine oxidation, and dioxidation. 'Trypsin' was selected as enzyme, and three miscleavages were also allowed. Mass accuracy was set to 300 ppm and 0.6 Da for MS and MS/MS mode, respectively. Protein identification was considered as unambiguous when a minimum of two peptides matched with a minimum score of 20. False discovery rates were also estimated using a reverse database as decoy.

As well as carrying out analysis of variance for the two populations combined, we also ran separate analyses of variance for each population. The overall effect of temperature, P_{CO_2} and their interaction on protein abundance in each population were tested through permutational multivariate analysis of variance (Permanova) using the adonis2 function in vegan (https://cran.r-project.org/package=vegan). Then, separate ANOVAs were fitted for each protein considering the effects of temperature, P_{CO_2} and their interaction, with *P*-values adjusted using FDR. For all proteins with significant environmental effects (FDR<0.05), differences between the four treatments were quantified with *post hoc* tests in emmeans.

To provide a clearer view of population responses to environmental variation, we ran additional exploratory and statistical analyses for each population separately using differentially abundant and successfully annotated proteins from the combined population proteomic analysis. We initially looked for correlations among proteins using principal component analysis (PCA), carried out in R using the packages FactoMineR (https://cran.r-project.org/package=FactoMineR; Lê et al., 2008) and factoextra (https://cran.r-project.org/package=factoextra), with spot size data scaled to unit variance. Correlations between proteins were identified by high loading values (>0.65 or <−0.65) of these variables onto principal components, which were visualised with vector plots. Differences between treatments were then visualised with individual coordinate plots and 95% confidence ellipses (the multidimensional space in which we expect to find the mean 95% of the time, given the underlying distribution of the data).

RESULTS

Differences in survival

Survival was significantly higher among Norwegian spat compared with French spat (χ^2=154.22, d.f.=1, *P*<0.0001). For Norwegian spat, temperature, P_{CO_2} and their interaction did not affect survival. For French spat, P_{CO_2} did not affect survival (as a main effect or through its interaction with temperature); however, temperature did have a significant effect (χ^2=18.79, d.f.=1, *P*<0.0001) and relative to spat reared at 13°C, mortality was higher at 16°C (*z-ratio*=−3.736, *P*=0.0005) and 19°C (*z*=−3.869, *P*=0.0003). Survival did not differ between the 16°C and 19°C treatments (*z*=−0.273, *P*=0.9597). Survival curves are shown in Fig. 1.

Variation in whole-organism phenotypes

Effects of P_{CO_2} and temperature on the three primary traits of shell height, dry body mass and total shell mass, differed markedly between French and Norwegian spat. However, for all three phenotypic traits and in both populations, initial height was a highly significant covariate (*P*<0.0001). Among French spat, none of the primary traits responded strongly to temperature (Table 2; Fig. 2A,C,E) and although elevated P_{CO_2} had a positive effect on dry body mass (*F*=4.92, d.f.=1, *P*=0.041), it did not influence shell height or total shell mass. On the other hand, P_{CO_2} effects were much stronger among Norwegian spat, where they interacted with initial height and temperature (Table 2). For shell height, the P_{CO_2}×temperature interaction was significant during the model selection process [in which maximum likelihood (ML) estimates were used; *F*=5.40, d.f.=2, *P*=0.014], but the interaction was not significant once optimal models were refitted using restricted maximum likelihood (REML) estimates (*F*=3.71, d.f.=2, *P*=0.055). However, the fact that the effects of temperature and P_{CO_2} appear similar for all three primary traits in Norwegian spat (Fig. 2B,D,F) suggests that the P_{CO_2}×temperature interaction for shell height, although weak, may be biologically meaningful. Thus, we report the P_{CO_2}-dependent temperature contrasts and temperature-dependent P_{CO_2} contrasts for all three traits in Table S1. At 19°C, elevated P_{CO_2} had a significant negative effect on both shell height (*t*=2.68, d.f.=11.9, *P*=0.020) and dry body mass (*t*=2.42, d.f.=11.6, *P*=0.033) and the effect was marginally non-significant for total shell mass (*t*=2.12, d.f.=11.7, *P*=0.056). In contrast, at 13°C, elevated P_{CO_2} resulted in a greater total shell mass (*t*=−2.24, d.f.=12.8, *P*=0.043). Furthermore, at elevated P_{CO_2}, there was a decrease in dry body mass at 19°C relative to 13°C (*t*=3.75, d.f. 12.0, *P*=0.007) and at normal P_{CO_2} there was an increase in total shell mass at 16°C relative to 13°C (*t*=−2.664, d.f. 13.2, *P*=0.0474).

Although condition index (CI) was based on the ratio of two of the primary traits (dry body mass over total shell mass), it revealed new effects that were not identified from analyses of primary traits. Specifically, analysis of CI identified a significant temperature effect in both French (Fig. 2G; *F*=5.90, d.f.=2, *P*=0.014) and Norwegian spat (Fig. 2H; *F*=16.63, d.f.=2, *P*<0.001), with CI declining as temperature increased, particularly when comparing 13°C and 19°C treatments (Table 2, Table S1). CI also responded positively to elevated P_{CO_2} in French spat (*F*=16.92, d.f.=1, *P*=0.001), mirroring the result found in dry body mass. Furthermore, initial height was not a significant covariate in explaining CI for Norwegian spat and had a weaker effect than temperature and P_{CO_2} among French spat (*F*=4.94, d.f.=1, *P*=0.027).

Metabolic rate differences

French spat had higher average oxygen consumption ($\dot{M}_{O_2}$) than Norwegian spat (91.98 µmol O_2 h^{-1} mg^{-1} compared with 78.20 µmol O_2 h^{-1} mg^{-1}); however, a three-way interaction between population, P_{CO_2} and temperature (*F*=7.79, d.f.=1, *P*<0.0076) suggested the environmental effects differed strongly between populations and models were refitted for each population separately. Among French spat, $\dot{M}_{O_2}$ was significantly higher in elevated P_{CO_2} treatments (*F*=41.67, d.f.=1, *P*<0.0001), but there was no effect of temperature (*F*=0.44, d.f.=1, *P*=0.516) nor any interaction between P_{CO_2} and temperature (*F*=0.51, d.f.=1, *P*=0.483). Among Norwegian spat, the interaction between

Journal of Experimental Biology (2023) 226, jeb245383. doi:10.1242/jeb.245383

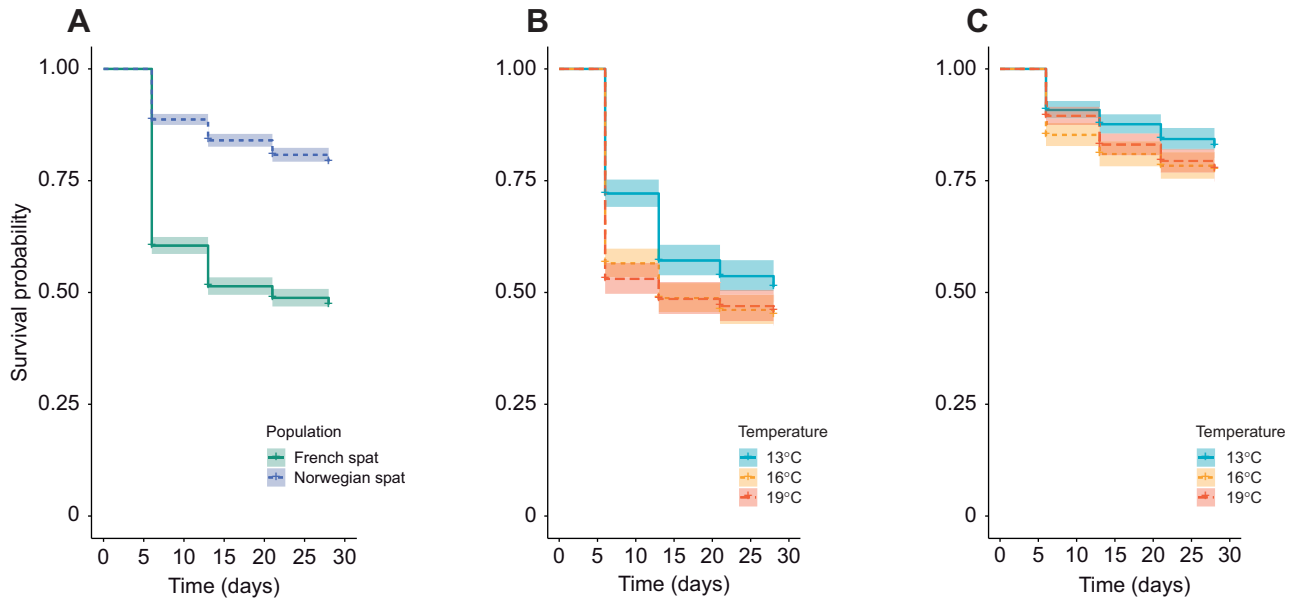

Fig. 1. Effect of temperature and pH on survival in French and Norwegian great scallop. (A) French (green, *n*=2556) and Norwegian (blue, *n*=2556) spat survival. French spat had significantly lower survival compared with Norwegian spat (χ^2=154.22, d.f.=1, *P*<0.0001). (B) Among French spat, increasing temperature (13°C, *n*=829; 16°C, *n*=922; 19°C, *n*=805) resulted in reduced survival (χ^2=18.79, *P*<0.0001). (C) Among Norwegian spat (13°C, *n*=882; 16°C, *n*=759; 19°C, *n*=915), temperature effects on survival were not significant (χ^2=2.29, *P*=0.319).

P_{CO_2} and temperature was significant (*F*=5.77, d.f.=1, *P*=0.025): pairwise *post hoc* Wilcoxon rank sum tests confirmed that $\dot{M}_{O_2}$ was significantly elevated (*P*<0.05) in the 13°C normal CO_2 treatment compared with the other treatments. Differences in $\dot{M}_{O_2}$ between treatments are summarised in Fig. 3.

Differential accumulation of proteins: combined population analysis

We identified 279 proteins common to all gels using SameSpots. Of these, 103 differed significantly in intensity (FDR<0.05) between populations (*n*=87), temperature treatments (*n*=17) or P_{CO_2} treatments (*n*=3); three differed according to two or more of these variables. Following mass spectrometry of these proteins, 79 were identified based on comparison with the protein database: 71 differed according to population, 8 differed according to temperature and 2 differed according to P_{CO_2} (two proteins differed according to two variables). These proteins are presented in Table S2 and Fig. 4. Of the 79 proteins, 23 were highly differentially accumulated (fold change>2) and 33 were moderately differentially accumulated (fold change>1.5). Two proteins

Table 2. Summary of effects and interactions of temperature, P_{CO_2} and initial height on organismal phenotypes in minimal models following backwards stepwise term-deletion

Trait	Spat population	Variable	Mean squares	d.f.	Den. d.f.*	*F*	*P*-value
Final shell height	French	Initial height	42.087	1	201.67	83.21	<0.0001
	Norwegian	Initial height	726.090	1	209.98	1508.91	<0.0001
		P_{CO_2}	4.580	1	204.03	9.51	0.0023
		Temperature	0.490	2	12.38	1.02	0.3896
		Initial height×P_{CO_2}	3.810	1	209.98	7.91	0.0054
		P_{CO_2}×Temperature	1.780	2	12.38	3.71	0.0548
Dry body mass	French	Initial height	5.005	1	202.86	45.28	<0.0001
		P_{CO_2}	0.544	1	16.24	4.92	0.0411
	Norwegian	Initial height	53.945	1	210.65	573.48	<0.0001
		P_{CO_2}	0.849	1	204.30	9.02	0.0030
		Temperature	0.336	2	12.14	3.58	0.0601
		Initial height×P_{CO_2}	0.762	1	210.65	8.11	0.0049
		P_{CO_2}×Temperature	0.386	2	12.14	4.10	0.0435
Total shell mass	French	Initial height	6.870	1	199.85	104.89	<0.0001
	Norwegian	Initial height	51.551	1	210.76	1373.80	<0.0001
		P_{CO_2}	0.515	1	204.36	13.72	0.0003
		Temperature	0.027	2	12.24	0.71	0.5105
		Initial height×P_{CO_2}	0.491	1	210.76	13.08	0.0004
		P_{CO_2}×Temperature	0.210	2	12.24	5.60	0.0187
Condition index	French	Initial height	0.0002	1	198.52	4.94	0.0274
		P_{CO_2}	0.0006	1	13.94	16.92	0.0011
		Temperature	0.0002	2	14.31	5.90	0.0136
	Norwegian	Temperature	0.0008	2	14.85	14.63	0.0003

*Den. d.f., denominator degrees of freedom.

Journal of Experimental Biology (2023) 226, jeb245383. doi:10.1242/jeb.245383

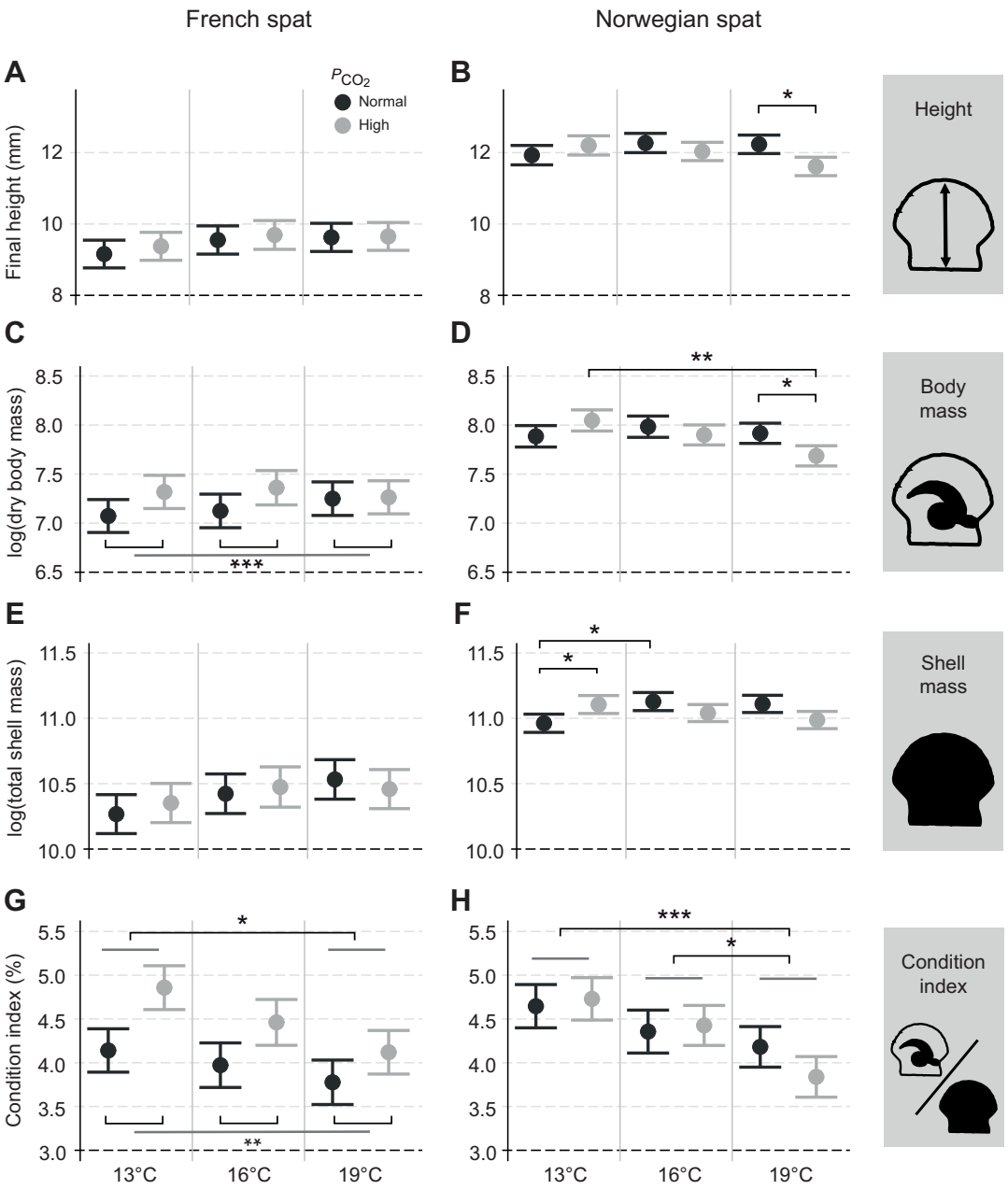

Fig. 2. Effect of temperature and pH on French and Norwegian scallop whole-organism phenotypic traits. (A,B) Final shell height. (C,D) Dry body mass (plotted as log of mass in μg). (E,F) Total shell mass (plotted as log of mass in μg). (G,H) Condition index. Values are mean-centred model estimates (±c.i.) derived from linear models considering initial height, temperature, pH, and all their interactions. Effect/interaction significance was determined by term deletion and model comparison, and estimated marginal means were used to determine significant temperature and temperature×P_{CO_2} contrasts. Simple brackets show temperature×P_{CO_2} interactions, brackets linking grey bars show temperature effects (G,H) and grey bars show P_{CO_2} effects (C,G). For French spat, n=36, 34, 35, 35, 33, 37; for Norwegian spat, n=35, 35, 34, 39, 38, 40. All statistical tests are shown in Table 2; *P<0.05, ***P<0.01, ***P<0.005.

annotated as 'uncharacterised' were further investigated using nucleic acid homology searches. Spot 447 (*Mizuhopecten yessoensis* locus 110464099) showed strong amino acid similarity (65.14%, *E*=7e-101) to the *Crassostrea gigas* cytoskeletal protease kyphoscoliosis peptidase (KY), while spot 468 (*Mizuhopecten yessoensis* locus 110453073) contained a conserved domain with significant similarity (interval 47–194, *E*=4.19e-07) to von Willebrand factor A domain (vWA), an extracellular glycoprotein.

Seventy-one of the 79 proteins differed significantly between populations, and the majority of these (43) were different isoforms of actin: 24 isoforms were elevated among French spat, and 19 were elevated among Norwegian spat (see fig. A4 in figshare: doi:10.6084/m9.figshare.22226239.v3). Actin isoforms were spread widely across the 2-DE gel and those that were more abundant in Norwegian spat generally had a higher pH and/or higher molecular weight. Another group of structural proteins which differed between the populations were motor proteins: 8 isoforms of myosin and 2 of paramyosin showed higher accumulation in Norwegian spat compared with French spat.

Of the 26 remaining proteins, the majority (18/26) differed between populations, and almost all of these (17/18) were more abundant in French spat than Norwegian spat: just one (gelsolin)

Journal of Experimental Biology (2023) 226, jeb245383. doi:10.1242/jeb.245383

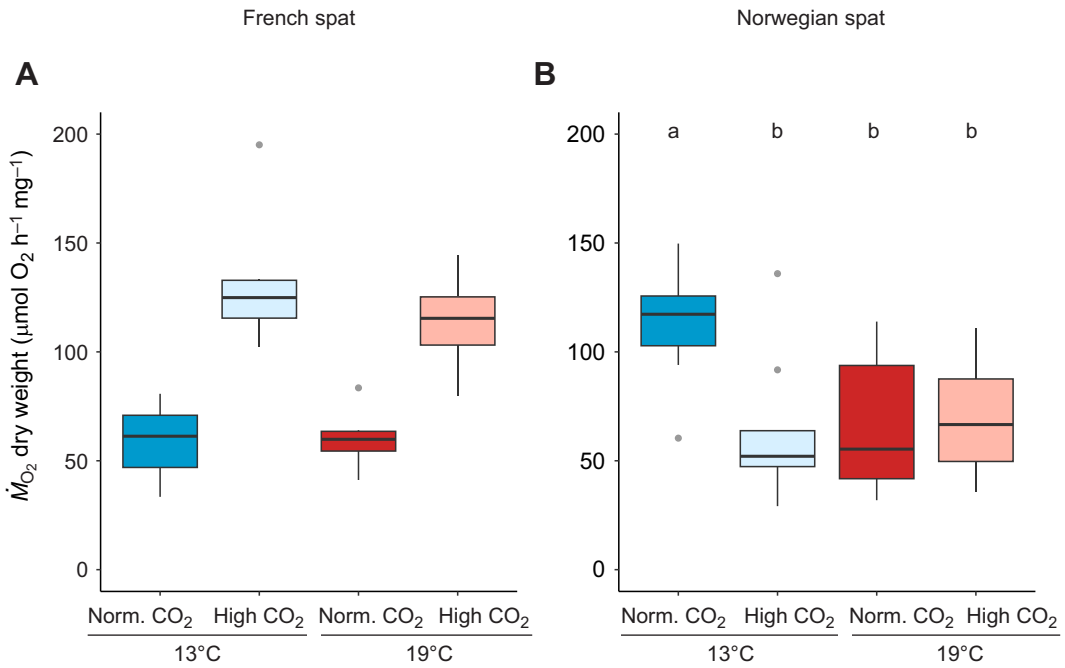

Fig. 3. Mass-corrected oxygen consumption ($\dot{M}_{O_2}$) in French and Norwegian spat after 5 weeks at experimental temperature and P_{CO_2}. French spat (A) displayed increased oxygen consumption under elevated P_{CO_2} (F=41.67, P<0.0001; n=7, 6, 6, 8). Among Norwegian spat (B), there was a significant interaction between elevated temperature and P_{CO_2} (F=5.77, P=0.025; n=7, 8, 6, 6). *Post hoc* tests (letters a,b) revealed that increases in temperature and/or P_{CO_2} result in reduced oxygen consumption.

showed higher accumulation in Norwegian spat. Nine proteins showed significant temperature and/or P_{CO_2} effects in the combined population analysis and five of these displayed fold changes greater than 1.5 (Fig. 5). The oxidative stress response protein manganese superoxide dismutase (MnSOD) was more abundant at 19°C (F=14.90, d.f.=1, FDR=0.008). Conversely, the extracellular matrix protein ependymin-related 1 (EPDR), mitochondrial complex I (complex I) and the molecular chaperone peptidyl-prolyl cis-trans isomerase (PPIase) were more abundant at 13°C (EPDR: F=21.94, d.f.=1, FDR=0.001; complex I: F=16.08, d.f.=1, FDR=0.005; PPIase: F=19.85, d.f.=1 FDR=0.002). An isoform of paramyosin was more abundant at elevated P_{CO_2} (F=9.30, d.f.=1, FDR=0.040) as well as being more abundant in Norwegian spat (F=10.18, d.f.=1, FDR=0.033).

Differential accumulation of proteins: separated population analyses

The Permanova revealed that both temperature (F=3.0444, d.f.=1, P=0.002) and P_{CO_2} (F=3.3187, d.f.=1, P=0.007) significantly influenced overall patterns of protein abundance in French spat but not Norwegian spat (temperature: F=0.6211, d.f.=1, P=0.721; P_{CO_2}: F=0.4765, d.f.=1, P=0.860). The interaction between temperature and P_{CO_2} was not significant for either population. Among French spat, individual ANOVAs for the 79 proteins revealed 12 with potential temperature or P_{CO_2} effects (FDR<0.05; Fig. 6; Table S3), six of which were also significant in the combined population analysis. Fold changes were greater than 1.5 in eight of these proteins. Although none of the 12 proteins showed a significant response to either temperature or P_{CO_2} at our statistical threshold (FDR<0.05), differing responses to elevated temperature and P_{CO_2} were suggested by *post hoc* tests (Table S4). These showed that elevated temperature and P_{CO_2} either had opposite effects that offset each other when combined (Fig. 6A–G), or similar effects that exacerbated one another additively (Fig. 6H,I). Conversely, among Norwegian spat, only 11 proteins showed potential responses to temperature, P_{CO_2} or their interaction (P<0.05; Fig. S2) and none of these were significant following correction for multiple testing (FDR<0.05).

The 12 environmentally dependent proteins in French scallops were ATP synthase, triosephosphate isomerase (TPI), medium-chain specific acyl-CoA dehydrogenase (ACAD), complex I, Retinal dehydrogenase 2 (RALDH2), MnSOD, PPIase, EPDR, an isoform of actin, an isoform of myosin, and putative isoforms of kyphoscoliosis peptidase (KY) and von Willebrand factor type A (vWA). For these 12 proteins, only one main effect, temperature (9/12) or P_{CO_2} (3/12), was significant at our stringent statistical cut-off (FDR<0.05). Despite this, *post hoc* tests indicated that both variables frequently had an impact on protein abundance (Table S3). For seven proteins (Fig. 6A–G), the most significant difference in abundance occurred between 13-highCO_2 and 19-normCO_2 treatments, while the comparison of 13-normCO_2 and 19-highCO_2 did not differ significantly. This suggests that P_{CO_2} and temperature had opposite effects that offset each other when both were elevated. For all these proteins (except ACAD, Fig. 6A), increasing temperature had a positive effect on abundance while elevated P_{CO_2} had a negative effect. On the other hand, in two proteins (complex I and PPIase; Fig. 6H,I) the 13-normCO_2 and 19-highCO_2 treatments differed the most, suggesting that temperature and P_{CO_2} both had additive negative effects on abundance.

Principal component analyses of protein abundance

To further explore correlations in protein abundance we carried out PCA using the 25 proteins that were not annotated as actin, myosin or paramyosin. Correlations were stronger among French spat, where the first two principal components (PC1 and PC2) together explained 54.7% of the total variance (Fig. 7A) compared with 44.5% in Norwegian spat (Fig. 7B). Among French spat, 12 proteins had high loading values (>0.65 or <−0.65) for PC1

Journal of Experimental Biology (2023) 226, jeb245383. doi:10.1242/jeb.245383

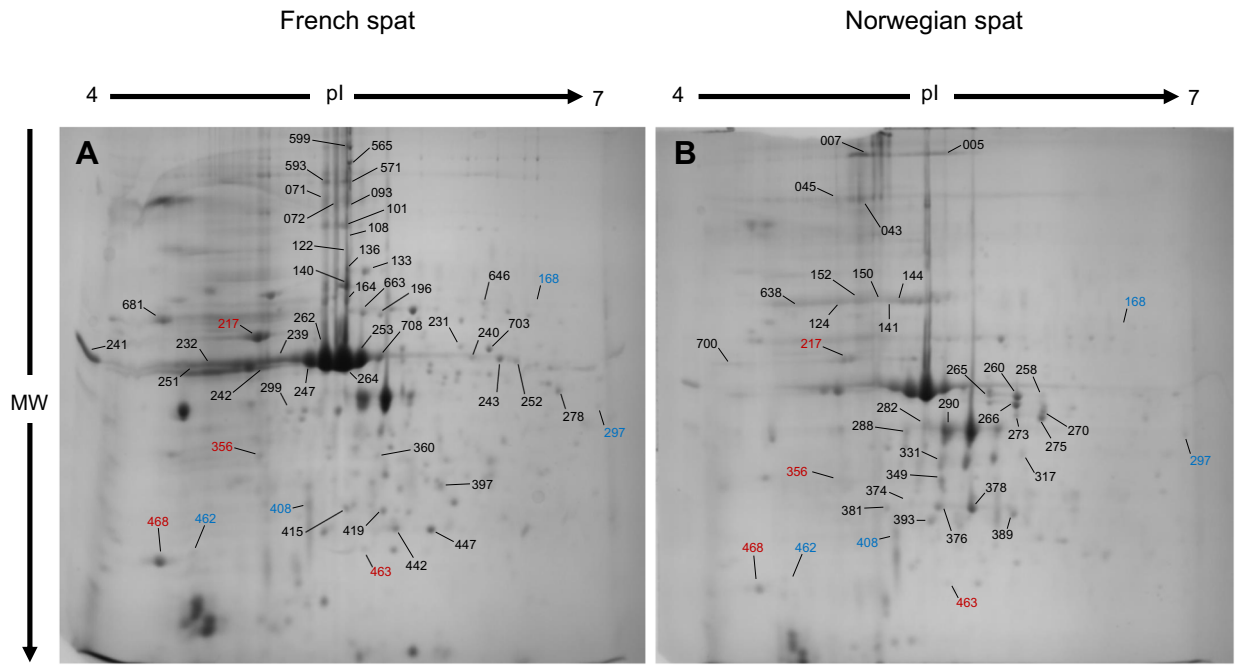

Fig. 4. Representative annotated 2-dimensional gel electrophoresis gel images. (A) French and (B) Norwegian (B) spat proteomes at 19°C and ambient P_{CO_2}. Proteins that were significantly more abundant in French spat are labelled (black numbers) in A; proteins that were significantly more abundant in Norwegian spat are labelled (black numbers) in B. Proteins with temperature-dependent abundance appear in both A and B. Protein spots that were more abundant at 19°C (both populations) are labelled in red, those that were more abundant at 13°C (both populations) are labelled in blue. MW, molecular weight; pI, isoelectric point.

(Fig. 7A), and treatments also showed separation along this axis in the individual coordinate plot (Fig. 7C). The confidence ellipse for 19-normCO_2 treatment was associated with higher PC1 values than any other treatment and the confidence ellipse for 13-highCO_2 treatment was associated with lower PC1 values than ellipses for either 19-normCO_2 or 19-highCO_2. Transaldolase (TALDO), TPI_1, TPI_2, ATP synthase, RALDH1, RALDH2, glutathione S-transferase (GST), KY and vWA were positively correlated with PC1, while glucose-6-phosphate isomerase (GPI), ACAD and an isoform of NADP-dependent isocitrate dehydrogenase (IDH_1) were negatively correlated with PC1. Among Norwegian spat, nine proteins had high loading values for PC1 (Fig. 7B), but there was no separation of treatments in the individual coordinate plot (Fig. 7D).

DISCUSSION

Phenotypic responses to environmental variation

Elevated temperature and P_{CO_2} treatments both had significant antagonistic consequences for growth phenotypes in Norwegian scallops, with the strongest effects on growth experienced when both stresses were combined, agreeing with previous results in scallops (Artigaud et al., 2014a; Alma et al., 2020). In contrast, growth of French spat was influenced less by experimental treatments: the only primary phenotypic trait affected was dry body mass, which increased in elevated P_{CO_2} treatments. However, elevated temperature resulted in greater mortality of French spat, suggesting a potential trade-off between growth and survival. While *P. maximus* adults have been shown to be fairly tolerant to warming and hypercapnic stresses (Götze et al., 2020), our results suggest that spat may pay some costs under OAW: reduced survival in the French spat experiencing warming and reduced growth in the Norwegian population experiencing acidification and warming.

Interestingly, condition index (CI; dry body mass divided by total shell mass), also revealed a clear positive effect of elevated P_{CO_2} in French spat. Similar results have previously been interpreted as seasonal shifts in patterns of resource allocation (Cameron et al., 2019) or subtle shifts in allocation to soft tissue and shell (Hiebenthal et al., 2013), but this result could also be an experimental artefact. It is possible that elevated P_{CO_2} resulted in some microalgal growth (tanks were only semi-open) and increased food availability. However, if this were the case, only French scallops were able to exploit it, as neither dry body mass nor CI increased at elevated P_{CO_2} in Norwegian spat. For scallops from both populations, CI declined with increasing temperatures in line with previously reported results from bivalves (Clark et al., 2013; Hiebenthal et al., 2013; Cameron et al., 2019; Pereira et al., 2020). This could be due to differences in the energetic costs of calcification compared with homeostasis: saturation states of aragonite and calcite increase at higher temperatures, potentially reducing the cost of calcification (Clark, 2020; Clark et al., 2020). Furthermore, as ectotherms approach their upper thermal limits, aerobic scope is reduced (Pörtner and Farrell, 2008; Sokolova et al., 2012), which can result in increased costs of basal metabolism and a relative decline in allocation of resources to soft tissue growth.

Metabolic responses to increasing temperature and P_{CO_2}

As ectotherms approach upper thermal limits, they may reduce their metabolic rates (Anestis et al., 2008; Clark et al., 2013), which could help to explain why oxygen consumption of Norwegian scallops declined at higher temperatures. In contrast, oxygen consumption was not influenced by temperature in French scallops, suggesting that these spat successfully acclimated to experimental temperatures to maintain metabolism (Seebacher et al., 2010). Although oxygen consumption of French scallops did not vary according to temperature, there was a clear increase in oxygen consumption at

Journal of Experimental Biology (2023) 226, jeb245383. doi:10.1242/jeb.245383

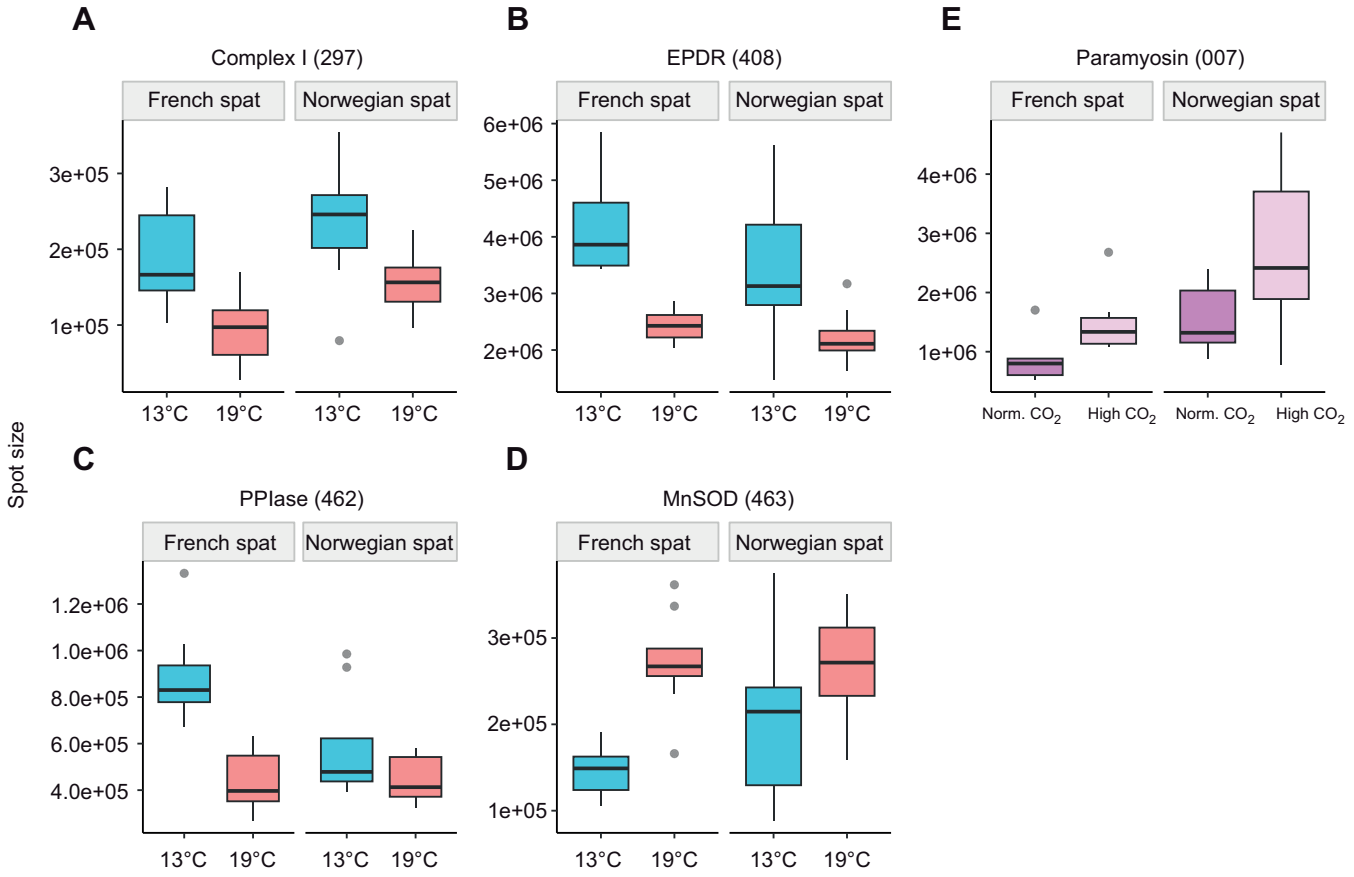

Fig. 5. Proteins that differed significantly between temperature and P_{CO_2} treatments in the combined population analysis (FDR<0.05, fold change>1.5). For temperature responses (A–D) protein spot size from both P_{CO_2} treatments are combined and for P_{CO_2} responses (E), protein spots from both temperatures are combined (in all cases n=8). (A) Complex I was more abundant at lower temperatures (F=16.08, FDR=0.005), as were (B) EPDR (F =21.94, FDR=0.001) and (C) PPIase (F=19.85, FDR=0.002). (D) MnSOD was less abundant at lower temperatures (F=14.90, FDR=0.008). (E) A paramyosin isoform was more abundant at elevated P_{CO_2} (F=9.30, FDR=0.040) and in Norwegian spat (F=10.18, d.f.=1, FDR=0.033). Numbers refer to labels on 2-DE protein spots in Fig. 4. complex I, mitochondrial complex I; EPDR, ependymin-related 1; MnSOD, manganese superoxide dismutase; PPIase, peptidyl-prolyl cis-trans isomerase.

elevated P_{CO_2}. This result mirrors findings in several other marine invertebrate species (Parker et al., 2012; Benítez et al., 2018; Harianto et al., 2021; Jiang et al., 2021), where increased $\dot{M}O2$ in response to increased P_{CO_2} appears to maintain cellular homeostasis. In contrast, Norwegian scallops reduced their oxygen consumption under elevated P_{CO_2} irrespective of temperature. Given that this response occurred at 13°C, which Norwegian scallops experience during the summer, it could indicate alternative strategies for dealing with P_{CO_2} variation between the populations, or that scallops from the Bay of Brest are better adapted to the more variable P_{CO_2} levels that occur there (Salt et al., 2016). Genetic variation in ability to acclimate to elevated P_{CO_2} has been observed previously among different selected lines of oysters (Parker et al., 2012) and mussels (Stapp et al., 2017), in which families tolerant of P_{CO_2} variation were found to increase metabolic rates under elevated P_{CO_2}, while sensitive families did not. Given the strong and significant genetic differentiation between French and Norwegian scallop populations (Morvezen et al., 2016; Vendrami et al., 2019), it seems likely that higher temperatures and P_{CO_2} in the Bay of Brest have led to an adaptive ability to acclimate to these conditions.

Proteomic responses to environmental variation

Variation in the influence of temperature and P_{CO_2} on metabolism was also detected in the proteome. While both populations responded to increased temperatures with increased abundance in the oxidative stress enzyme MnSOD and reduced abundance of the oxidative phosphorylation enzyme mitochondrial complex I (also known as quinone oxidoreductase and NADH dehydrogenase), the proteome of French spat showed far greater plasticity than that of Norwegian spat, again highlighting potential evolutionary differences between the populations. Among French spat, temperature effects were generally greater than P_{CO_2} effects, but acidification frequently exerted a subtle effect in the opposite direction to heating, with increased temperature and P_{CO_2} offsetting one another. This was emphasised by the PCA, in which increasing temperature had a positive effect on the first principal component, and increasing P_{CO_2} had a negative effect. Four energy metabolism proteins (TALDO, TPI_1, TPI_2, and ATP-synthase) had positive loadings with PC1, and three energy metabolism proteins (GPI, IDH_1 and ACAD) had negative loadings. A decrease in GPI (the first enzyme involved in glycolysis) and concurrent increase in the pentose phosphate pathway (PPP) enzyme TALDO indicates a putative shift from the preparatory phase of glycolysis to the oxidative phase of PPP (Krüger et al., 2011). Furthermore, a greater abundance of TPI isoforms indicates that PPP metabolites are likely returning to the pay-off phase of glycolysis rather than being recycled between oxidative and non-oxidative branches of the PPP (as this would

Journal of Experimental Biology (2023) 226, jeb245383. doi:10.1242/jeb.245383

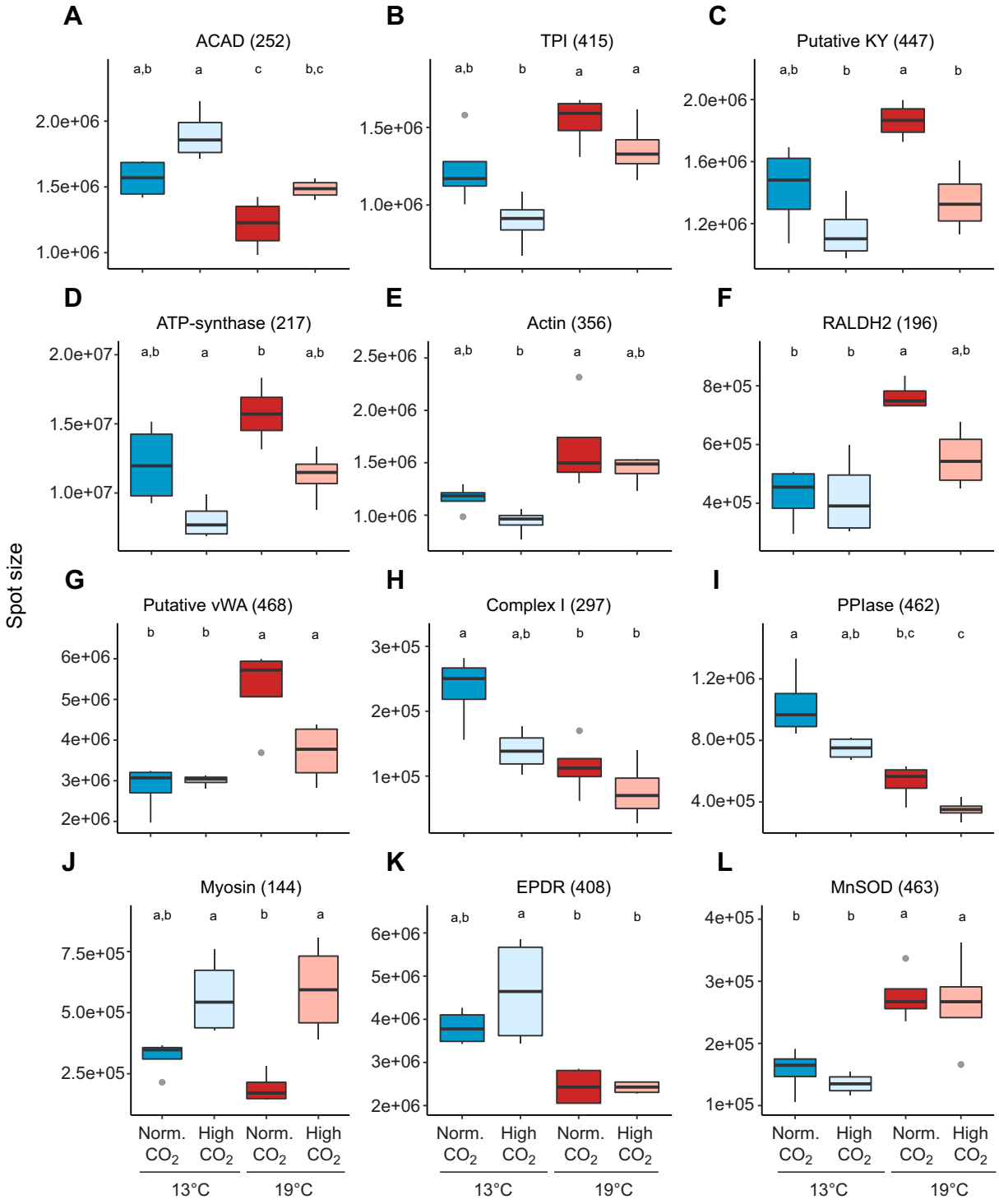

Fig. 6. Proteins that differed significantly according to temperature or P_{CO_2} in French spat (FDR<0.05). Temperature effects (A-B,E-L) were more prevalent than P_{CO_2} (C,D), effects, although *post hoc* test results (indicated by letters above plots) suggest that in many cases both were responsible for shaping protein abundance. ANOVA statistics are provided in Table S3, *post hoc* test statistics are provided in Table S4. For all treatments in all proteins, *n*=4. ACAD, acyl-CoA dehydrogenase; Putative KY, putative isoform of kyphoscoliosis peptidase; RALDH2, retinal dehydrogenase 2; TPI, triosephosphate isomerase; Putative vWA, putative isoform of von Willebrand factor type A.

also require GPI; Krüger et al., 2011). TPI may be a particularly strong marker of this metabolic change because of its tendency to oligomerise at higher temperatures (Katebi and Jernigan, 2014; Rodríguez-Bolaños et al., 2020). By directing carbon metabolism to the oxidative branch of the PPP, French scallops may be generating greater quantities of the reducing agent NADPH (Ralser et al., 2007; Stincone et al., 2015) to mitigate the increase in reactive oxygen species (ROS) production associated with metabolism at higher temperatures (Tomanek and Zuzow, 2010). This idea is supported by a positive correlation in the abundance of

Journal of Experimental Biology (2023) 226, jeb245383. doi:10.1242/jeb.245383

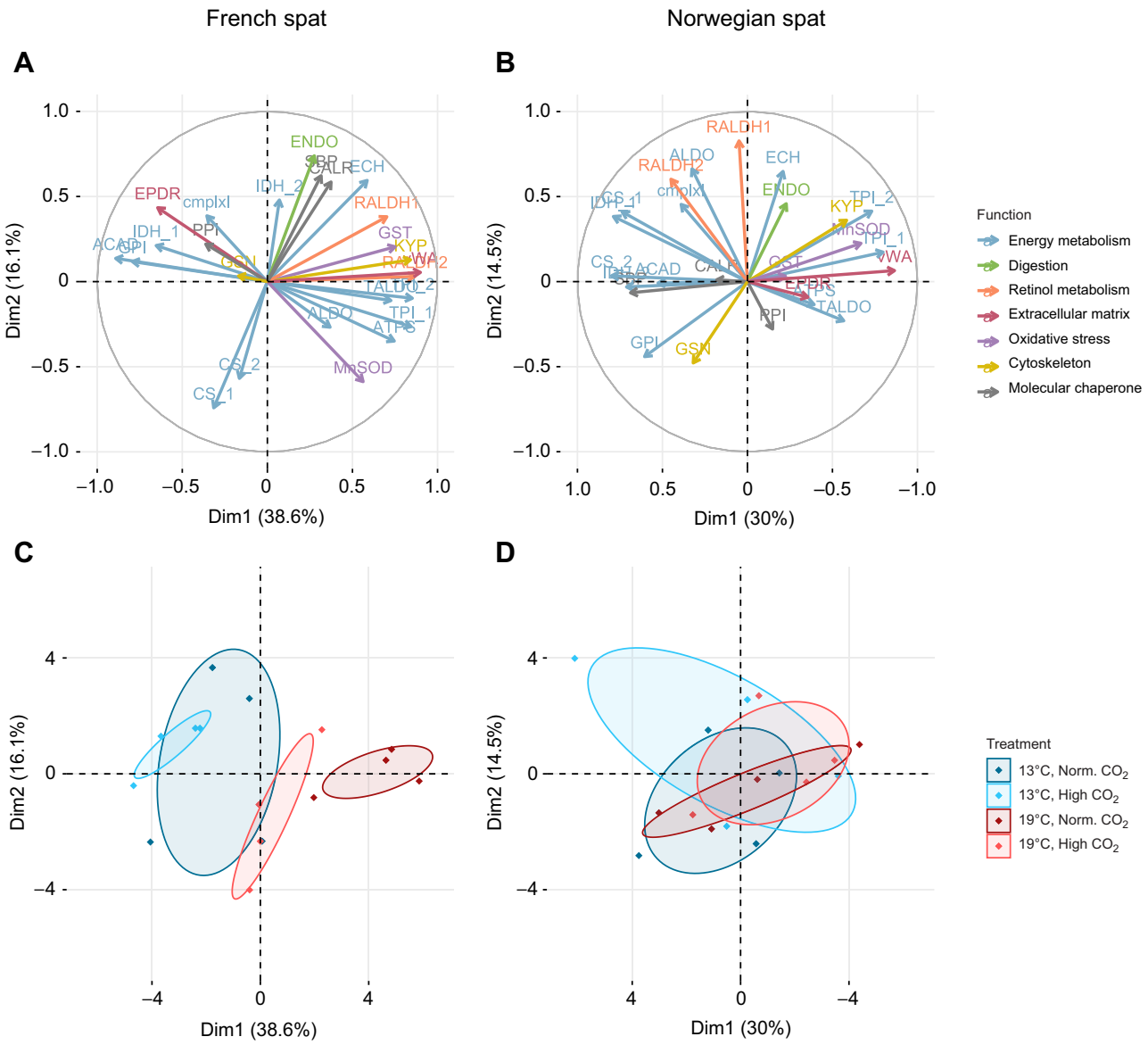

Fig. 7. Vector and PCA plots of all proteins that were not actin, myosin or paramyosin. Vector plots show that patterns of protein correlation were stronger in French (A) than Norwegian (B) spat. Proteins are coloured according to their (putative) function. Most protein abbreviations are in text, and a full list is found in Table S2. PCA plots show greater separation of treatments for French (C) than Norwegian (D) spat (95% confidence ellipses coloured according to temperature and P_{CO_2} treatment). In both plots of Norwegian spat proteins (B and D), PC1 has been inverted to highlight similarities between the populations. For all treatments in all proteins, n=4. CALR, calreticulin; CS1/2, citrate synthase 1/2; ECH, enoyl-CoA hydratase; GPI, glucose-6-phosphate isomerase; GSN, gelsolin; GST, glutathione *S*-transferase; IDH1/2, isocitrate dehydrogenase 1/2; KYP, putative isoform of kyphoscoliosis peptidase; cmplxI, mitochondrial complex I; TALDO, transaldolase; ATPS, ATP-synthase; SBP, selenium-binding protein; ALDO, fructose-bisphosphate aldolase; ENDO, endoglucanase.

the antioxidant GST, which is another critical component in managing ROS stress (Park et al., 2019).

Four other proteins (RALDH1, RALDH2, KY and vWA) with putative roles in development, growth and biomineralization also had high positive loadings for PC1 (increased abundance at high temperature, reduced abundance in elevated P_{CO_2}) in French scallops. Retinal dehydrogenases (RALDH1 and RALDH2) are involved in retinoic acid metabolism, which is associated with embryonic development, organ generation and homeostasis in vertebrates (Marlétaz et al., 2006), but are also known to affect development of the molluscan central nervous system (Carter et al., 2010, 2015). Kyphoscoliosis peptidase (KY) has previously been linked to molluscan stress responses (Chaney and Gracey, 2011; Shiel et al., 2017; Blalock et al., 2020), but may also play a role in muscle growth (Shen et al., 2018). Finally the extracellular matrix protein vWA is likely to be involved in biomineralization (Funabara et al., 2014; Chandra Rajan and Vengatesen, 2020; Clark et al., 2020). Beyond these results in French scallops, two other proteins with putative roles in biomineralization (EPDR and PPIase) were found to be more abundant at 13°C in the combined population analysis. EPDR has been directly implicated in molluscan biomineralization (Jackson et al., 2006; Marie et al., 2010; Miyamoto et al., 2013), while a subfamily of PPIases known as cyclophilins facilitate molluscan nacre formation (Jackson et al., 2010; Marie et al., 2013). Both temperature and P_{CO_2} are known to have important effects on biomineralization processes and the

crystalline structure of calcium carbonate (Fitzer et al., 2015), and our results provide some indications of the proteins that may underlie such changes.

Population differences in cytoskeletal proteins

The structural proteins actin and myosin were among the most numerous in our study. Although actin has previously been implicated in bivalve physiological stress responses to both temperature (Tomanek et al., 2011) and P_{CO_2} (Moreira et al., 2018), we found just one environmentally responsive isoform of actin that positively responded to increased temperature in French spat. Instead, actin isoforms differed substantially between the populations, with some more abundant in French scallops and others more abundant in Norwegian scallops, echoing an earlier *in natura* comparison of adult *P. maximus* from these two populations (Artigaud et al., 2014b): results from our common garden approach provide more evidence that differences in proteomic abundance reflect divergent genetic backgrounds. Actin is abundant and multifunctional (Dominguez and Holmes, 2011). Its density in our samples may be due to its presence in the scallop's largest organ, the adductor muscle (Chantler, 2006), where it aids with muscular contraction through its interaction with myosin. Indeed, eight isoforms of myosin and two of the related protein paramyosin (both components of the adductor muscle; Chantler, 2006) also showed strong population differentiation. However, unlike actin, these proteins were always more abundant in Norwegian spat. As they grow, scallop spat increasingly use their adductor muscle for swimming, which can lead to an increase in muscle condition (Kleinman et al., 1996). This could explain why Norwegian scallops (which were slightly older and larger at the start of the experiment) had elevated levels of these proteins. While no isoforms of myosin or paramyosin responded to temperature treatment, there was some evidence of P_{CO_2} sensitivity in one isoform of myosin (more abundant at elevated P_{CO_2} in French spat) and one isoform of paramyosin (more abundant at elevated P_{CO_2} in the combined population analysis). Several recent studies from diverse marine invertebrates have linked increases in myosin and/or paramyosin transcript (Wäge et al., 2016; Bailey et al., 2017) and protein (Timmins-Schiffman et al., 2014; Zhao et al., 2020) abundance with the response to elevated P_{CO_2}. While the mechanism by which myosin and paramyosin abundance aids the response to acidification remains unclear, its presence in diverse taxa could suggest an evolutionary conserved physiological response.

Integrating results across biological scales and conclusions

Drawing on phenotypic results from whole organismal, metabolic and proteomic scales, we show clear differences in how French and Norwegian *Pecten maximus* spat respond to increases in temperature and P_{CO_2}. Although some proteomic and organismal responses were common to both populations, such as the increase in MnSOD and decrease in the abundance of complex I at high temperature, and the corresponding decline in CI, French spat seem to acclimate better to temperature and P_{CO_2} variation and more precisely adjust their energy metabolism than Norwegian spat. By putatively altering their carbon metabolism to deal with increased redox stress associated with higher temperatures, and by increasing oxygen consumption at elevated P_{CO_2}, which potentially maintains cellular homeostasis, French spat appear better able to maintain growth under OAW conditions. In contrast, Norwegian spat did not appear to fine-tune their proteome, but reduced oxygen consumption if temperature or P_{CO_2} increased. This corresponded with negative effects on growth, with reduced body mass and shell height when high temperature and P_{CO_2} were combined.

The experiments were carried out during July, when SST in the Bay of Brest (northwest France) is slightly higher (16.7°C) than in the North Sea near the western fjords of Norway (15.9°C), which could help to explain why metabolic rates and growth phenotypes of French spat were not adversely affected by temperature. Furthermore, P_{CO_2} tends to be higher and more variable in the Bay of Brest (Salt et al., 2016; Omar et al., 2019), and French spat increased their metabolism and maintained growth under elevated P_{CO_2}. This increased plasticity in French spat may reflect adaptation to higher mean temperatures and more variable P_{CO_2} conditions in the Bay of Brest, while the more stable P_{CO_2} conditions under which Norwegian scallops have evolved may limit their ability to adapt to rapid environmental change. However, these metabolic adjustments may be difficult to maintain over longer periods: Harianto et al. (2021) found that urchins exposed to elevated P_{CO_2} and high temperatures after 4 weeks increased metabolism (similar to the French spat in our study), but that after 12 weeks, the combined stress led to reduced metabolism. The costs of maintaining metabolic function and growth at elevated temperatures could also have contributed towards the reduced survival we observed in French spat. These two populations are known to be genetically divergent (Morvezen et al., 2016), with some genetic differentiation at loci associated with environmental variation in mean annual SST and dissolved organic carbon (Vendrami et al., 2019). This could therefore suggest some adaptive differentiation of these scallop populations in response to environmental variation.

Among marine invertebrate ectotherms, traits as diverse as size (Kelly et al., 2013), metabolic rate (Wood et al., 2016; Osores et al., 2017), developmental plasticity (Pereira et al., 2017), feeding rates (Vargas et al., 2017) and growth (Pespeni et al., 2013a) show important inter-population differences when key environmental factors such as temperature and P_{CO_2} vary. Our integrative approach helps to disentangle some of the molecular and metabolic differences between populations of this economically important species, highlighting which physiological processes may be involved in acclimatization. Future experiments that combine these approaches with genetic studies that estimate the population-specific heritability and plasticity of acclimatory or adaptive traits will be essential in improving our understanding of how populations will respond to global climate change.

Acknowledgements

We are grateful to Florian Breton from L'Écloserie du Tinduff and to Thorolf Magnesen from Scalpro AS for supplying spat. We thank Julien Thébault for use of the Zeiss Stereomicroscope and Axiovision software. Thanks also to Steven Parratt for discussion about statistical approaches.

Competing interests

The authors declare no competing or financial interests.

Author contributions

Conceptualization: E.H., V.P., P.B., G.C.; Methodology: E.H., S.P.S.R., S.A., P.M., P.B.; Validation: E.H.; Formal analysis: E.H., S.P.S.R., S.A., B.B.; Investigation: E.H., S.P.S.R., S.A., J.P., B.B., P.M.; Resources: E.H., S.P.S.R., S.A., P.M., V.P., O.S., P.B.; Writing - original draft: E.H., S.P.S.R., S.A., B.B.; Writing - review & editing: E.H., S.P.S.R., S.A., V.P., O.S., P.B., G.C.; Visualization: E.H.; Supervision: E.H., S.A., V.P., O.S., P.B., G.C.; Project administration: E.H., G.C.; Funding acquisition: E.H., V.P., O.S., P.B., G.C.

Funding

This work was supported by a grant from the Regional Council of Brittany, from the European Regional Development Fund (ERDF), and by the Agence Nationale de la

Recherche “Laboratoire d’Excellence” LabexMER (ANR-10-LABX-19) through a grant from the French government under the program “Investissements d’Avenir”. The project was also supported by state funding to the ISblue interdisciplinary graduate school for the blue planet (ANR-17-EURE-0015), also under the program “Investissements d’Avenir” and within the framework of France 2030. Additional funding was provided by the Institute of Marine Research (Havforskningsinstituttet) through the project “Ecological interactions of low trophic benthic production” (82120-01).

Data availability

The data that support the findings of this study, including an appendix of additional figures are available through figshare (doi:10.6084/m9.figshare.22226239).

References

Alma, L., Kram, K. E., Holtgrieve, G. W., Barbarino, A., Fiamengo, C. J. and Padilla-Gamiño, J. L. (2020). Ocean acidification and warming effects on the physiology, skeletal properties, and microbiome of the purple-hinge rock scallop. *Comp. Biochem. Physiol. Part A Mol. Integr. Physiol.* **240**, 110579. doi:10.1016/j.cbpa.2019.110579

Anestis, A., Pörtner, H.-O., Lazou, A. and Michaelidis, B. (2008). Metabolic and molecular stress responses of sublittoral bearded horse mussel *Modiolus barbatus* to warming sea water: Implications for vertical zonation. *J. Exp. Biol.* **211**, 2889-2898. doi:10.1242/jeb.016782

Artigaud, S., Lacroix, C., Pichereau, V. and Flye-Sainte-Marie, J. (2014a). Respiratory response to combined heat and hypoxia in the marine bivalves *Pecten maximus* and *Mytilus* spp. *Comp. Biochem. Physiol. Part A Mol. Integr. Physiol.* **175**, 135-140. doi:10.1016/j.cbpa.2014.06.005

Artigaud, S., Lavaud, R., Thébault, J., Jean, F., Strand, Ø., Strohmeier, T., Milan, M. and Pichereau, V. (2014b). Proteomic-based comparison between populations of the great scallop, *Pecten maximus*. *J. Proteomics* **105**, 164-173. doi:10.1016/j.jprot.2014.03.026

Artigaud, S., Thorne, M. A. S., Richard, J., Lavaud, R., Jean, F., Flye-Sainte-Marie, J., Peck, L. S., Pichereau, V. and Clark, M. S. (2014c). Deep sequencing of the mantle transcriptome of the great scallop *Pecten maximus*. *Mar. Genomics* **15**, 3-4. doi:10.1016/j.margen.2014.03.006

Artigaud, S., Richard, J., Thorne, M. A. S., Lavaud, R., Flye-Sainte-Marie, J., Jean, F., Peck, L. S., Clark, M. S. and Pichereau, V. (2015). Deciphering the molecular adaptation of the king scallop (*Pecten maximus*) to heat stress using transcriptomics and proteomics. *BMC Genomics* **16**, 988. doi:10.1186/s12864-015-2132-x

Bailey, A., De Wit, P., Thor, P., Browman, H. I., Bjelland, R., Shema, S., Fields, D. M., Runge, J. A., Thompson, C. and Hop, H. (2017). Regulation of gene expression is associated with tolerance of the Arctic copepod *Calanus glacialis* to CO2-acidified sea water. *Ecol. Evol.* **7**, 7145-7160. doi:10.1002/ece3.3063

Bates, D. M., Maechler, M., Bolker, B. and Walker, S. (2015). Fitting linear mixed-effects models using lme4. *J. Stat. Softw.* **67**, 1-48. doi:10.18637/jss.v067.i01.

Benítez, S., Lagos, N. A., Osores, S. J. A., Opitz, T., Duarte, C., Navarro, J. M. and Lardies, M. A. (2018). High pCO2 levels affect metabolic rate, but not feeding behavior and fitness, of farmed giant mussel *Choromytilus chorus*. *Aquac. Environ. Interact.* **10**, 267-278. doi:10.3354/aei00271

Benson, B. B. and Krause Jr, D. (1984). The concentration and isotopic fractionation of oxygen dissolved in freshwater and seawater in equilibrium with the atmosphere 1. *Limnol. Oceanog.* **29**, 620-632.

Blalock, B. J., Robinson, W. E. and Poynton, H. C. (2020). Assessing legacy and endocrine disrupting pollutants in Boston Harbor with transcriptomic biomarkers. *Aquat. Toxicol.* **220**, 105397. doi:10.1016/j.aquatox.2019.105397

Brierley, A. S. and Kingsford, M. J. (2009). Impacts of climate change on marine organisms and ecosystems. *Curr. Biol.* **19**, R602-R614. doi:10.1016/j.cub.2009.05.046

Byrne, M. (2011). Impact of ocean warming and ocean acidification on marine invertebrate life history stages: vulnerabilities and potential for persistence in a changing ocean. *Oceanogr. Mar. Biol. An Annu. Rev.* **49**, 1-42.

Byrne, M. (2012). Global change ecotoxicology: Identification of early life history bottlenecks in marine invertebrates, variable species responses and variable experimental approaches. *Mar. Environ. Res.* **76**, 3-15. doi:10.1016/j.marenvres.2011.10.004

Cai, W.-J. and Wang, Y. (1998). The chemistry, fluxes, and sources of carbon dioxide in the estuarine waters of the Satilla and Altamaha Rivers, Georgia. *Limnol. Oceanogr.* **43**, 657-668. doi:10.4319/lo.1998.43.4.0657

Caldeira, K. and Wickett, M. E. (2003). Anthropogenic carbon and ocean pH. *Nature* **425**, 365. doi:10.1038/425365a

Calosi, P., Melatunan, S., Turner, L. M., Artioli, Y., Davidson, R. L., Byrne, J. J., Viant, M. R., Widdicombe, S. and Rundle, S. D. (2017). Regional adaptation defines sensitivity to future ocean acidification. *Nat. Commun.* **8**, 13994. doi:10.1038/ncomms13994

Cameron, L. P., Reymond, C. E., Müller-Lundin, F., Westfield, I., Grabowski, J. H., Westphal, H. and Ries, J. B. (2019). Effects of temperature and ocean acidification on the extrapallial fluid pH, calcification rate, and condition factor of the king scallop *Pecten maximus*. *J. Shellfish Res.* **38**, 763-777. doi:10.2983/035.038.0327

Carter, C. J., Farrar, N., Carlone, R. L. and Spencer, G. E. (2010). Developmental expression of a molluscan RXR and evidence for its novel, nongenomic role in growth cone guidance. *Dev. Biol.* **343**, 124-137. doi:10.1016/j.ydbio.2010.03.023

Carter, C. J., Rand, C., Mohammad, I., Lepp, A., Vesprini, N., Wiebe, O., Carlone, R. and Spencer, G. E. (2015). Expression of a retinoic acid receptor (RAR)-like protein in the embryonic and adult nervous system of a protostome species. *J. Exp. Zool. Part B Mol. Dev. Evol.* **324**, 51-67. doi:10.1002/jez.b.22604

Chandra Rajan, K. and Vengatesen, T. (2020). Molecular adaptation of molluscan biomineralisation to high-CO2 oceans – The known and the unknown. *Mar. Environ. Res.* **155**, 104883. doi:10.1016/j.marenvres.2020.104883

Chaney, M. L. and Gracey, A. Y. (2011). Mass mortality in Pacific oysters is associated with a specific gene expression signature. *Mol. Ecol.* **20**, 2942-2954. doi:10.1111/j.1365-294X.2011.05152.x

Chantler, P. D. (2006). Scallop adductor muscles: structure and function. In *Scallops: Biology, Ecology and Aquaculture* (ed. S. E. Shumway and G. J. Parsons), pp. 229-316. Amsterdam: Elsevier B.V.

Chauvaud, L., Patry, Y., Jolivet, A., Cam, E., Le Goff, C., Strand, Ø., Charrier, G., Thébault, J., Lazure, P., Gotthard, K. et al. (2012). Variation in size and growth of the Great Scallop *Pecten maximus* along a latitudinal gradient. *PLoS ONE* **7**, e37717. doi:10.1371/journal.pone.0037717

Christophersen, G., Román, G., Gallagher, J. and Magnesen, T. (2008). Post-transport recovery of cultured scallop (*Pecten maximus*) spat, juveniles and adults. *Aquac. Int.* **16**, 171-185. doi:10.1007/s10499-007-9135-9

Clark, M. S. (2020). Molecular mechanisms of biomineralization in marine invertebrates. *J. Exp. Biol.* **223**, jeb206961. doi:10.1242/jeb.206961

Clark, M. S., Thorne, M. A. S., Amaral, A., Vieira, F., Batista, F. M., Reis, J. and Power, D. M. (2013). Identification of molecular and physiological responses to chronic environmental challenge in an invasive species: The Pacific oyster, *Crassostrea gigas*. *Ecol. Evol.* **3**, 3283-3297. doi:10.1002/ece3.719

Clark, M. S., Peck, L. S., Arivalagan, J., Backeljau, T., Berland, S., Cardoso, J. C. R., Caurcel, C., Chapelle, G., De Noia, M., Dupont, S. et al. (2020). Deciphering mollusc shell production: the roles of genetic mechanisms through to ecology, aquaculture and biomimetics. *Biol. Rev.* **95**, 1812-1837. doi:10.1111/brv.12640

Crowley, T. J. and Berner, R. A. (2001). CO2 and climate change. *Science* **292**, 870-872. doi:10.1126/science.1061664

Dam, H. G. (2013). Evolutionary adaptation of marine zooplankton to global change. *Ann. Rev. Mar. Sci.* **5**, 349-370. doi:10.1146/annurev-marine-121211-172229

Dam, H. G., deMayo, J. A., Park, G., Norton, L., He, X., Finiguerra, M. B., Baumann, H., Brennan, R. S. and Pespeni, M. H. (2021). Rapid, but limited, zooplankton adaptation to simultaneous warming and acidification. *Nat. Clim. Chang.* **11**, 780-786. doi:10.1038/s41558-021-01131-5

Davis, A. R., Coleman, D., Broad, A., Byrne, M., Dworjanyn, S. A. and Przeslawski, R. (2013). Complex responses of intertidal molluscan embryos to a warming and acidifying ocean in the presence of UV radiation. *PLoS One* **8**, e55939. doi:10.1371/journal.pone.0055939

Di Santo, V. (2016). Intraspecific variation in physiological performance of a benthic elasmobranch challenged by ocean acidification and warming. *J. Exp. Biol.* **219**, 1725-1733. doi:10.1242/jeb.139204

Dominguez, R. and Holmes, K. C. (2011). Actin structure and function. *Annu. Rev. Biophys.* **40**, 169-186. doi:10.1146/annurev-biophys-042910-155359

Doney, S. C., Fabry, V. J., Feely, R. A. and Kleypas, J. A. (2009). Ocean acidification: the other CO_2 problem. *Ann. Rev. Mar. Sci.* **1**, 169-192. doi:10.1146/annurev.marine.010908.163834

Duncan, P. F., Brand, A. R., Strand, Ø. and Foucher, E. (2016). Chapter 19 - The European Scallop Fisheries for *Pecten maximus*, *Aequipecten opercularis*, *Chlamys islandica*, and *Mimachlamys varia*. In *Developments in Aquaculture and Fisheries Science* (ed. S. E. Shumway and G. J. Parsons), pp. 781-858. Amsterdam: Elsevier.

Fields, P. A., Zuzow, M. J. and Tomanek, L. (2012). Proteomic responses of blue mussel (*Mytilus*) congeners to temperature acclimation. *J. Exp. Biol.* **215**, 1106-1116. doi:10.1242/jeb.062273

Fitzer, S. C., Zhu, W., Tanner, K. E., Phoenix, V. R., Kamenos, N. A. and Cusack, M. (2015). Ocean acidification alters the material properties of *Mytilus edulis* shells. *J. R. Soc. Interface* **12**, 20141227. doi:10.1098/rsif.2014.1227

Fox, J. and Weisberg, S. (2011). *An R Companion to Applied Regression*, 2nd edn. Thousand Oaks, CA, USA.

Funabara, D., Ohmori, F., Kinoshita, S., Koyama, H., Mizutani, S., Ota, A., Osakabe, Y., Nagai, K., Maeyama, K., Okamoto, K. et al. (2014). Novel genes participating in the formation of prismatic and nacreous layers in the pearl oyster as revealed by their tissue distribution and RNA interference knockdown. *PLoS ONE* **9**, e84706. doi:10.1371/journal.pone.0084706

Götze, S., Bock, C., Eymann, C., Lannig, G., Steffen, J. B. M. and Pörtner, H.-O. (2020). Single and combined effects of the “Deadly trio” hypoxia, hypercapnia and warming on the cellular metabolism of the great scallop *Pecten maximus*. *Comp. Biochem. Physiol. Part B Biochem. Mol. Biol.* **243**, 110438. doi:10.1016/j.cbpb.2020.110438

Hale, S. S., Buffum, H. W., Kiddon, J. A. and Hughes, M. M. (2017). Subtidal benthic invertebrates shifting northward along the US Atlantic Coast. *Estuaries Coasts* **40**, 1744-1756. doi:10.1007/s12237-017-0236-z

Hansen, J., Sato, M., Ruedy, R., Lo, K., Lea, D. W. and Medina-Elizade, M. (2006). Global temperature change. *Proc. Natl. Acad. Sci. USA* **103**, 14288-14293. doi:10.1073/pnas.0606291103

Harianto, J., Aldridge, J., Torres Gabarda, S. A., Grainger, R. J. and Byrne, M. (2021). Impacts of acclimation in warm-low pH conditions on the physiology of the Sea Urchin *Heliocidaris erythrogramma* and carryover effects for juvenile offspring. *Front. Mar. Sci.* **7**, 588938. doi:10.3389/fmars.2020.588938

Harney, E. D., Artigaud, S., Le Souchu, P., Miner, P., Corporeau, C., Essid, H., Pichereau, V. and Nunes, F. L. D. (2016). Non-additive effects of ocean acidification in combination with warming on the larval proteome of the Pacific oyster, *Crassostrea gigas*. *J. Proteomics* **135**, 151-161. doi:10.1016/j.jprot.2015.12.001

Harvey, B. P., Gwynn-Jones, D. and Moore, P. J. (2013). Meta-analysis reveals complex marine biological responses to the interactive effects of ocean acidification and warming. *Ecol. Evol.* **3**, 1016-1030. doi:10.1002/ece3.516

Hiebenthal, C., Philipp, E. E. R., Eisenhauer, A. and Wahl, M. (2013). Effects of seawater pCO2 and temperature on shell growth, shell stability, condition and cellular stress of Western Baltic Sea *Mytilus edulis* (L.) and *Arctica islandica* (L.). *Mar. Biol.* **160**, 2073-2087. doi:10.1007/s00227-012-2080-9

Hurd, C. L., Beardall, J., Comeau, S., Cornwall, C. E., Havenhand, J. N., Munday, P. L., Parker, L. M., Raven, J. A. and Mcgraw, C. M. (2020). Ocean acidification as a multiple driver: How interactions between changing seawater carbonate parameters affect marine life. *Mar. Freshw. Res.* **71**, 263-274. doi:10.1071/MF19267

IPCC (2022). Climate Change 2022: Impacts, Adaptation, and Vulnerability (ed. H.-O. Pörtner, D. C. Roberts, M. Tignor, E. S. Poloczanska, K. Mintenbeck, A. Alegría, M. Craig, S. Langsdorf, S. Löschke, V. Möller, A. Okem and B. Rama). Cambridge, UK: Cambridge University Press.

Jackson, D. J., Mcdougall, C., Green, K., Simpson, F., Wörheide, G. and Degnan, B. M. (2006). A rapidly evolving secretome builds and patterns a sea shell. *BMC Biol.* **4**, 40. doi:10.1186/1741-7007-4-40

Jackson, D. J., McDougall, C., Woodcroft, B., Moase, P., Rose, R. A., Kube, M., Reinhardt, R., Rokhsar, D. S., Montagnani, C., Joubert, C. et al. (2010). Parallel evolution of nacre building gene sets in molluscs. *Mol. Biol. Evol.* **27**, 591-608. doi:10.1093/molbev/msp278

Jiang, W., Wang, X., Rastrick, S. P. S., Wang, J., Zhang, Y., Strand, Ø., Fang, J. and Jiang, Z. (2021). Effects of elevated pCO2 on the physiological energetics of Pacific oyster, *Crassostrea gigas*. *ICES J. Mar. Sci.* **78**, 2579-2590. doi:10.1093/icesjms/fsab139

Katebi, A. R. and Jernigan, R. L. (2014). The critical role of the loops of triosephosphate isomerase for its oligomerization, dynamics, and functionality. *Protein Sci.* **23**, 213-228. doi:10.1002/pro.2407

Kelly, M. W., Padilla-Gamiño, J. L. and Hofmann, G. E. (2013). Natural variation and the capacity to adapt to ocean acidification in the keystone sea urchin *Strongylocentrotus purpuratus*. *Glob. Chang. Biol.* **19**, 2536-2546. doi:10.1111/gcb.12251

Kleinman, S., Hatcher, B. G. and Scheibling, R. E. (1996). Growth and content of energy reserves in juvenile sea scallops, *Placopecten magellanicus*, as a function of swimming frequency and water temperature in the laboratory. *Mar. Biol.* **124**, 629-635. doi:10.1007/BF00351044

Kroeker, K. J., Kordas, R. L., Crim, R. N., Hendriks, I. E., Ramajo, L., Singh, G. S., Duarte, C. M. and Gattuso, J.-P. (2013). Impacts of ocean acidification on marine organisms: quantifying sensitivities and interaction with warming. *Glob. Chang. Biol.* **19**, 1884-1896. doi:10.1111/gcb.12179

Krüger, A., Grüning, N. M., Wamelink, M. M. C., Kerick, M., Kirpy, A., Parkhomchuk, D., Bluemlein, K., Schweiger, M. R., Soldatov, A., Lehrach, H. et al. (2011). The pentose phosphate pathway is a metabolic redox sensor and regulates transcription during the antioxidant response. *Antioxid. Redox Signal.* **15**, 311-324. doi:10.1089/ars.2010.3797

Lê, S., Josse, J. and Husson, F. (2008). FactoMineR: an R package for multivariate analysis. *J. Stat. Softw.* **25**, 1-18. doi:10.18637/jss.v025.i01

Lefevre, S. (2016). Are global warming and ocean acidification conspiring against marine ectotherms? A meta-analysis of the respiratory effects of elevated temperature, high CO2 and their interaction. *Conserv. Physiol.* **4**, cow009. doi:10.1093/conphys/cow009

Lucas, A. and Beninger, P. G. (1985). The use of physiological condition indices in marine bivalve aquaculture. *Aquaculture* **44**, 187-200. doi:10.1016/0044-8486(85)90243-1

Marie, B., Marie, A., Jackson, D. J., Dubost, L., Degnan, B. M., Milet, C. and Marin, F. (2010). Proteomic analysis of the organic matrix of the abalone *Haliotis asinina* calcified shell. *Proteome Sci.* **8**, 54. doi:10.1186/1477-5956-8-54

Marie, B., Jackson, D. J., Ramos-Silva, P., Zanella-Cléon, I., Guichard, N. and Marin, F. (2013). The shell-forming proteome of *Lottia gigantea* reveals both deep conservations and lineage-specific novelties. *FEBS J.* **280**, 214-232. doi:10.1111/febs.12062

Marlétaz, F., Holland, L. Z., Laudet, V. and Schubert, M. (2006). Retinoic acid signaling and the evolution of chordates. *Int. J. Biol. Sci.* **2**, 38-47. doi:10.7150/ijbs.2.38

Matoo, O. B., Ivanina, A. V., Ullstad, C., Beniash, E. and Sokolova, I. M. (2013). Interactive effects of elevated temperature and CO(2) levels on metabolism and oxidative stress in two common marine bivalves (*Crassostrea virginica* and *Mercenaria mercenaria*). *Comp. Biochem. Physiol. Part A Mol. Integr. Physiol.* **164**, 545-553. doi:10.1016/j.cbpa.2012.12.025

Miyamoto, H., Endo, H., Hashimoto, N., Limura, K., Isowa, Y., Kinoshita, S., Kotaki, T., Masaoka, T., Miki, T., Nakayama, S. et al. (2013). The diversity of shell matrix proteins: genome-wide investigation of the pearl oyster, *Pinctada fucata*. *Zoolog. Sci.* **30**, 801-816. doi:10.2108/zsj.30.801

Moreira, A., Figueira, E., Mestre, N. C., Schrama, D., Soares, A. M. V. M., Freitas, R. and Bebianno, M. J. (2018). Impacts of the combined exposure to seawater acidification and arsenic on the proteome of *Crassostrea angulata* and *Crassostrea gigas*. *Aquat. Toxicol.* **203**, 117-129. doi:10.1016/j.aquatox.2018.07.021

Morley, S. A., Lurman, G. J., Skepper, J. N., Pörtner, H.-O. and Peck, L. S. (2009). Thermal plasticity of mitochondria: a latitudinal comparison between Southern Ocean molluscs. *Comp. Biochem. Physiol. A Mol. Integr. Physiol.* **152**, 423-430. doi:10.1016/j.cbpa.2008.11.015

Morvezen, R., Charrier, G., Boudry, P., Chauvaud, L., Breton, F., Strand, Ø. and Laroche, J. (2015). Genetic structure of a commercially exploited bivalve, the great scallop *Pecten maximus*, along the European coasts. *Conserv. Genet.* **17**, 57-67. doi:10.1007/s10592-015-0760-y

Mykles, D. L., Ghalambor, C. K., Stillman, J. H. and Tomanek, L. (2010). Grand challenges in comparative physiology: integration across disciplines and across levels of biological organization. *Integr. Comp. Biol.* **50**, 6-16. doi:10.1093/icb/icq015

Noaman, N. and Coorssen, J. R. (2018). Coomassie does it (better): a Robin Hood approach to total protein quantification. *Anal. Biochem.* **556**, 53-56. doi:10.1016/j.ab.2018.05.012

Okazaki, R. R., Towle, E. K., Van Hooidonk, R., Mor, C., Winter, R. N., Piggot, A. M., Cunning, R., Baker, A. C., Klaus, J. S., Swart, P. K. et al. (2017). Species-specific responses to climate change and community composition determine future calcification rates of Florida Keys reefs. *Glob. Chang. Biol.* **23**, 1023-1035. doi:10.1111/gcb.13481

Omar, A. M., Thomas, H., Olsen, A., Becker, M., Skjelvan, I. and Reverdin, G. (2019). Trends of ocean Acidification and pCO2 in the Northern North Sea, 2003–2015. *J. Geophys. Res. Biogeosciences* **124**, 3088-3103. doi:10.1029/2018JG004992

Osores, S. J. A., Lagos, N. A., San Martín, V., Manríquez, P. H., Vargas, C. A., Torres, R., Navarro, J. M., Poupin, M. J., Saldías, G. S. and Lardies, M. A. (2017). Plasticity and inter-population variability in physiological and life-history traits of the mussel *Mytilus chilensis*: a reciprocal transplant experiment. *J. Exp. Mar. Bio. Ecol.* **490**, 1-12. doi:10.1016/j.jembe.2017.02.005

Park, J. C., Lee, M.-C., Yoon, D.-S., Han, J., Park, H. G., Hwang, U.-K. and Lee, J.-S. (2019). Genome-wide identification and expression of the entire 52 glutathione S-transferase (GST) subfamily genes in the Cu2+-exposed marine copepods *Tigriopus japonicus* and *Paracyclopina nana*. *Aquat. Toxicol.* **209**, 56-69. doi:10.1016/j.aquatox.2019.01.020

Parker, L. M., Ross, P. M., O'Connor, W. A., Borysko, L., Raftos, D. A. and Pörtner, H.-O. (2012). Adult exposure influences offspring response to ocean acidification in oysters. *Glob. Chang. Biol.* **18**, 82-92. doi:10.1111/j.1365-2486.2011.02520.x

Payne, N. L. and Smith, J. A. (2017). An alternative explanation for global trends in thermal tolerance. *Ecol. Lett.* **20**, 70-77. doi:10.1111/ele.12707

Pereira, R. J., Sasaki, M. C. and Burton, R. S. (2017). Adaptation to a latitudinal thermal gradient within a widespread copepod species: The contributions of genetic divergence and phenotypic plasticity. *Proc. R. Soc. B Biol. Sci.* **284**, 20170236. doi:10.1098/rspb.2017.0236

Pereira, R. R. C., Scanes, E., Gibbs, M., Byrne, M. and Ross, P. M. (2020). Can prior exposure to stress enhance resilience to ocean warming in two oyster species? *PLoS ONE* **15**, e0228527. doi:10.1371/journal.pone.0228527

Pespeni, M. H., Barney, B. T. and Palumbi, S. R. (2013a). Differences in the regulation of growth and biomineralization genes revealed through long-term common-garden acclimation and experimental genomics in the purple sea Urchin. *Evolution (N. Y)* **67**, 1901-1914. doi:10.1111/evo.12036

Pespeni, M. H., Sanford, E., Gaylord, B., Hill, T. M., Hosfelt, J. D., Jaris, H. K., LaVigne, M., Lenz, E. A., Russell, A. D., Young, M. K. et al. (2013b). Evolutionary change during experimental ocean acidification. *Proc. Natl. Acad. Sci. USA* **110**, 1220673110. doi:10.1073/pnas.1220673110

Pörtner, H.-O. (2002). Climate variations and the physiological basis of temperature dependent biogeography: Systemic to molecular hierarchy of thermal tolerance in animals. *Comp. Biochem. Physiol. Part A Mol. Integr. Physiol.* **132**, 739-761. doi:10.1016/S1095-6433(02)00045-4

Pörtner, H.-O. (2012). Integrating climate-related stressor effects on marine organisms: unifying principles linking molecule to ecosystem-level changes. *Mar. Ecol. Prog. Ser.* **470**, 273-290. doi:10.3354/meps10123

Pörtner, H.-O. and Farrell, A. P. (2008). Physiology and climate change. *Science* **322**, 690-692. doi:10.1126/science.1163156

Pörtner, H.-O., Bennett, A. F., Bozinovic, F., Clarke, A., Lardies, M. A., Lucassen, M., Pelster, B., Schiemer, F. and Stillman, J. H. (2006). Trade-offs in thermal adaptation: the need for a molecular to ecological integration. *Physiol. Biochem. Zool.* **79**, 295-313. doi:10.1086/499986

Pörtner, H.-O., Dupont, S., Melzner, F., Storch, D. and Thorndyke, M. (2010). Studies of metabolic rate and other characters across life stages. In: *Guide to best practices for ocean acidification research and data reporting* (ed. L. Hansson, V. Fabry, J.-P. Gattuso, U. Riebesell), pp. 167-180. Publications Office of the European Union. https://data.europa.eu/doi/10.2777/58454

Ralser, M., Wamelink, M. M., Kowald, A., Gerisch, B., Heeren, G., Struys, E. A. et al. (2007). Dynamic rerouting of the carbohydrate flux is key to counteracting oxidative stress. *J. Biol.* **6**, 1-18.

Rastrick, S. P. S. and Whiteley, N. M. (2011). Congeneric amphipods show differing abilities to maintain metabolic rates with latitude. *Physiol. Biochem. Zool.* **84**, 154-165. doi:10.1086/658857

Rastrick, S. P. S. and Whiteley, N. M. (2013). Influence of natural thermal gradients on whole animal rates of protein synthesis in marine gammarid amphipods. *PLoS ONE* **8**, e60050. doi:10.1371/journal.pone.0060050

Rastrick, S. P. S., Collier, V., Graham, H., Strohmeier, T., Whiteley, N. M., Strand, Ø. and Woodson, C. B. (2018). Feeding plasticity more than metabolic rate drives the productivity of economically important filter feeders in response to elevated CO2 and reduced salinity. *ICES J. Mar. Sci.* **75**, 2117-2128. doi:10.1093/icesjms/fsy079

Rheuban, J. E., Doney, S. C., Cooley, S. R. and Hart, D. R. (2018). Projected impacts of future climate change, ocean acidification, and management on the US Atlantic sea scallop (*Placopecten magellanicus*) fishery. *PLoS ONE* **13**, e0203536. doi:10.1371/journal.pone.0203536

Ries, J. B., Cohen, A. L. and Mccorkle, D. C. (2009). Marine calcifiers exhibit mixed responses to CO2-induced ocean acidification. *Geology* **37**, 1131-1134. doi:10.1130/G30210A.1

Rodríguez-Bolaños, M., Miranda-Astudillo, H., Pérez-Castañeda, E., González-Halphen, D. and Perez-Montfort, R. (2020). Native aggregation is a common feature among triosephosphate isomerases of different species. *Sci. Rep.* **10**, 1338. doi:10.1038/s41598-020-58272-4

Sabine, C. L., Feely, R. A., Gruber, N., Key, R. M., Lee, K., Bullister, J. L., Wanninkhof, R., Wong, C. S., Wallace, D. W. R., Tilbrook, B. et al. (2004). The oceanic sink for anthropogenic CO2. *Science* **305**, 367-371. doi:10.1126/science.1097403

Salt, L. A., Beaumont, L., Blain, S., Bucciarelli, E., Grossteffan, E., Guillot, A., L'helguen, S., Merlivat, L., Répécaud, M., Quéméner, L. et al. (2016). The annual and seasonal variability of the carbonate system in the Bay of Brest (Northwest Atlantic Shelf, 2008–2014). *Mar. Chem.* **187**, 1-15. doi:10.1016/j.marchem.2016.09.003

Sanford, E. and Kelly, M. W. (2011). Local adaptation in marine invertebrates. *Ann. Rev. Mar. Sci.* **3**, 509-535. doi:10.1146/annurev-marine-120709-142756

Scanes, E., Parker, L. M., O'Connor, W. A. and Ross, P. M. (2014). Mixed effects of elevated pCO2 on fertilisation, larval and juvenile development and adult responses in the mobile subtidal scallop *Mimachlamys asperrima* (Lamarck, 1819). *PLoS ONE* **9**, e93649. doi:10.1371/journal.pone.0093649

Schalkhausser, B., Bock, C., Stemmer, K., Brey, T., Pörtner, H.-O. and Lannig, G. (2013). Impact of ocean acidification on escape performance of the king scallop, *Pecten maximus*, from Norway. *Mar. Biol.* **160**, 1995-2006. doi:10.1007/s00227-012-2057-8

Schalkhausser, B., Bock, C., Pörtner, H.-O. and Lannig, G. (2014). Escape performance of temperate king scallop, *Pecten maximus* under ocean warming and acidification. *Mar. Biol.* **161**, 2819-2829. doi:10.1007/s00227-014-2548-x

Seebacher, F., Brand, M. D., Else, P. L., Guderley, H., Hulbert, A. J. and Moyes, C. D. (2010). Plasticity of oxidative metabolism in variable climates: Molecular mechanisms. *Physiol. Biochem. Zool.* **83**, 721-732. doi:10.1086/649964

Seebacher, F., White, C. R. and Franklin, C. E. (2015). Physiological plasticity increases resilience of ectothermic animals to climate change. *Nat. Clim. Chang.* **5**, 61-66. doi:10.1038/nclimate2457

Shen, M., Di, G., Li, M., Fu, J., Dai, Q., Miao, X., Huang, M., You, W. and Ke, C. (2018). Proteomics Studies on the three Larval Stages of Development and Metamorphosis of *Babylonia areolata*. *Sci. Rep.* **8**, 6269. doi:10.1038/s41598-018-24645-z

Shiel, B. P., Hall, N. E., Cooke, I. R., Robinson, N. A. and Strugnell, J. M. (2017). Epipodial tentacle gene expression and predetermined resilience to summer mortality in the commercially important greenlip abalone, *Haliotis laevigata*. *Mar. Biotechnol.* **19**, 195-205. doi:10.1007/s10126-017-9742-z

Small, D. P., Milazzo, M., Bertolini, C., Graham, H., Hauton, C., Hall-Spencer, J. M., Rastrick, S. P. S. and Pl, D. (2015). Sensitivity in Natural Systems. *Ices J. Mar. Sci.* **73**, 1-9.

Sokolova, I. M., Frederich, M., Bagwe, R., Lannig, G. and Sukhotin, A. A. (2012). Energy homeostasis as an integrative tool for assessing limits of environmental stress tolerance in aquatic invertebrates. *Mar. Environ. Res.* **79**, 1-15. doi:10.1016/j.marenvres.2012.04.003

Stapp, L. S., Thomsen, J., Schade, H., Bock, C., Melzner, F., Pörtner, H.-O. and Lannig, G. (2017). Intra-population variability of ocean acidification impacts on the physiology of Baltic blue mussels (*Mytilus edulis*): integrating tissue and organism response. *J. Comp. Physiol. B Biochem. Syst. Environ. Physiol.* **187**, 529-543. doi:10.1007/s00360-016-1053-6

Stincone, A., Prigione, A., Cramer, T., Wamelink, M. M., Campbell, K., Cheung, E. et al. (2015). The return of metabolism: biochemistry and physiology of the pentose phosphate pathway. *Biol. Rev.* **90**, 927-963. doi:10.1111/brv.12140

Sunday, J. M., Bates, A. E. and Dulvy, N. K. (2011). Global analysis of thermal tolerance and latitude in ectotherms. *Proc. R. Soc. B Biol. Sci.* **278**, 1823-1830. doi:10.1098/rspb.2010.1295

Timmins-Schiffman, E. B., Coffey, W. D., Hua, W., Nunn, B. L., Dickinson, G. H. and Roberts, S. B. (2014). Shotgun proteomics reveals physiological response to ocean acidification in *Crassostrea gigas*. *BMC Genomics* **15**, 951. doi:10.1186/1471-2164-15-951

Timmins-Schiffman, E. B., Guzmán, J. M., Elliott Thompson, R., Vadopalas, B., Eudeline, B. and Roberts, S. B. (2020). Dynamic response in the larval geoduck (*Panopea generosa*) proteome to elevated pCO2. *Ecol. Evol.* **10**, 185-197. doi:10.1002/ece3.5885

Todgham, A. E. and Stillman, J. H. (2013). Physiological responses to shifts in multiple environmental stressors: Relevance in a changing world. *Integr. Comp. Biol.* **53**, 539-544. doi:10.1093/icb/ict086

Tomanek, L. (2011). Environmental proteomics: changes in the proteome of marine organisms in response to environmental stress, pollutants, infection, symbiosis, and development. *Ann. Rev. Mar. Sci.* **3**, 373-399. doi:10.1146/annurev-marine-120709-142729

Tomanek, L. (2014). Proteomics to study adaptations in marine organisms to environmental stress. *J. Proteomics* **105**, 92-106. doi:10.1016/j.jprot.2014.04.009

Tomanek, L. and Zuzow, M. J. (2010). The proteomic response of the mussel congeners *Mytilus galloprovincialis* and *M. trossulus* to acute heat stress: implications for thermal tolerance limits and metabolic costs of thermal stress. *J. Exp. Biol.* **213**, 3559-3574. doi:10.1242/jeb.041228

Tomanek, L., Zuzow, M. J., Ivanina, A. V., Beniash, E. and Sokolova, I. M. (2011). Proteomic response to elevated PCO_2 level in eastern oysters, *Crassostrea virginica*: evidence for oxidative stress. *J. Exp. Biol.* **214**, 1836-1844. doi:10.1242/jeb.055475

Vargas, C. A., Lagos, N. A., Lardies, M. A., Duarte, C., Manríquez, P. H., Aguilera, V. M., Broitman, B., Widdicombe, S. and Dupont, S. (2017). Species-specific responses to ocean acidification should account for local adaptation and adaptive plasticity. *Nat. Ecol. Evol.* **1**, 0084. doi:10.1038/s41559-017-0084

Vendrami, D. L. J., De Noia, M., Telesca, L., Handal, W., Charrier, G., Boudry, P., Eberhart-Phillips, L. and Hoffman, J. I. (2019). RAD sequencing sheds new light on the genetic structure and local adaptation of European scallops and resolves their demographic histories. *Sci. Rep.* **9**, 7455. doi:10.1038/s41598-019-43939-4

Wäge, J., Lerebours, A., Hardege, J. D. and Rotchell, J. M. (2016). Exposure to low pH induces molecular level changes in the marine worm, *Platynereis dumerilii*. *Ecotoxicol. Environ. Saf.* **124**, 105-110. doi:10.1016/j.ecoenv.2015.10.008

Whiteley, N. M., Rastrick, S. P. S., Lunt, D. H. and Rock, J. (2011). Latitudinal variations in the physiology of marine gammarid amphipods. *J. Exp. Mar. Bio. Ecol.* **400**, 70-77. doi:10.1016/j.jembe.2011.02.027

Wood, H. L., Sundell, K., Almroth, B. C., Sköld, H. N. and Eriksson, S. P. (2016). Population-dependent effects of ocean acidification. *Proc. R. Soc. B Biol. Sci.* **283**, 20160163. doi:10.1098/rspb.2016.0163

Zhao, X., Han, Y., Chen, B., Xia, B., Qu, K. and Liu, G. (2020). CO2-driven ocean acidification weakens mussel shell defense capacity and induces global molecular compensatory responses. *Chemosphere* **243**, 125415. doi:10.1016/j.chemosphere.2019.125415